Analysis of N^6-methyladenosine reveals a new important mechanism regulating the salt tolerance of sweet sorghum

Hongxiang Zheng[1], Xi Sun[1], Jinlu Li[1], Yushuang Song[1], Jie Song[1], Fang Wang[2], Luning Liu[3,4], Xiansheng Zhang[2], Na Sui[1]*

[1]Shandong Provincial Key Laboratory of Plant Stress, College of Life Sciences, Shandong Normal University, Jinan, Shandong, 250014, China.

[2]State Key Laboratory of Crop Biology, College of Life Sciences, Shandong Agricultural University, Taian, Shandong, 271018, China.

[3]College of Marine Life Sciences, and Frontiers Science Center for Deep Ocean Multispheres and Earth System, Ocean University of China, Qingdao 266003, China

[4]Institute of Integrative Biology, University of Liverpool, Liverpool L69 7ZB, United Kingdom

*Corresponding author. E-mail: suina@sdnu.edu.cn

Highlights

1. Most studies on m^6A in plants have focused on *Arabidopsis thaliana*, and this study is the first time to reveal the role of m^6A modification in crop for salt tolerance.
2. There are considerable differences in the m^6A modifications of sweet sorghum genotypes and *A. thaliana*. This difference in m^6A modifications may be one of the reasons for causing and maintaining differential salt tolerance.
3. The m^6A modification is highly complex and dynamic in the regulation of salt stress for sweet sorghum, but its regulating ability is limited by its own level of m^6A modification.
4. The number and extent of m^6A modification on salt-resistant transcripts can be used as a reference to assess the salt tolerance of crops.

Abstract

The N^6-methyladenosine (m^6A) modification is the most common internal post-transcriptional modification, with important regulatory effects on RNA export, splicing, stability, and translation. Studies on the m^6A modifications in plants have focused on *Arabidopsis thaliana* growth and development. However, *A. thaliana* is a salt-sensitive and model plant species. Thus, studies aimed at characterizing the role of the m^6A modification in the salt stress responses of highly salt-tolerant crop species are needed. Sweet sorghum is cultivated as an energy and forage crop, which is highly suitable for growth on saline-alkaline land. Exploring the m^6A modification in sweet sorghum may be important for elucidating the salt-resistance mechanism of crops. In this study, we mapped the m^6A modifications in two sorghum genotypes (salt-tolerant M-81E and salt-sensitive Roma) that differ regarding salt tolerance. The m^6A modification in sweet sorghum under salt stress was drastically altered, especially in Roma, where the m^6A modification on mRNAs of some salt-resistant related transcripts increased, resulting in enhanced mRNA stability, which in turn was involved in the regulation of salt tolerance in sweet sorghum. Although m^6A modifications are important for regulating sweet sorghum salt tolerance, the regulatory activity is limited by the initial m^6A modification level. Additionally, in M-81E and Roma, the differences in the m^6A modifications were much greater than the differences in gene expression levels and are more sensitive. Our study suggests that the number and extent of m^6A modifications on the transcripts of salt-resistance genes may be important factors for determining and assessing the salt tolerance of crops.

***Keywords*:**

N^6-methyladenosine, post-transcriptional regulation, salt tolerance, sweet sorghum

1. Introduction

The N^6-methyladenosine (m^6A) modification is the most common type of eukaryotic mRNA modification and has been detected in numerous organisms [1-4]. In mammals, the m^6A modification is catalyzed by a methyltransferase complex consisting of METTL3 (MTase complex comprising methyltransferase-like 3) [5], WTAP (Wilms' tumor 1-associating protein) [6], and METTL14 (methyltransferase-like 14) [7]. This modification process is dynamic in the cell and is reversed by the demethylases FTO (fat mass and obesity-associated protein) [8] and ALKBH5 (α-ketoglutarate-dependent dioxygenase alkb homolog 5) [9]. Additionally, the m^6A-binding protein (also called readers) plays a specific regulatory role by recognizing the m^6A modification sites. The readers mainly include the YTH domain-containing protein YTHDF2 (DF2), YTHDF3 (DF3) [1], HNRNPA2B1 [6], and eIF3 (eukaryotic initiation factor 3) [10].

In *Arabidopsis thaliana*, many important biological processes require proper m^6A modifications [11]. MTA, MTB, and FIP37 are considered to form the main m^6A methyltransferase complex. The *METTL3* homolog *MTA* (At4g10760) is highly expressed in meristems and seeds, and a loss-of-function mutation to this gene results in a complete lack of m^6A as well as an embryonic lethal phenotype [12, 13]. Thus, m^6A modification is essential for embryo development. Previous studies have revealed that *FIP37* (At3g54170), a homolog of *WTAP* in humans and *Drosophila melanogaster*, interacts with MTA *in vitro* and *in vivo*. Mutants lacking *FIP37* undergo a substantial overproliferation of shoot apical meristems without aerial organs and a transcriptome-wide loss of m^6A modifications [14]. These observations suggest the m^6A modification is necessary for maintaining the continuous differentiation of shoot meristems. *MTB* (At4g09980) is a homolog of the human *METTL14* gene. The knockdown of *MTB* leads to a nearly 50% decrease in m^6A levels [15]. Studying plant demethylases can reveal the physiological effects of m^6A accumulation. The *ALKBH9B* (At2g17970) and *ALKBH10B* (At4g02940) genes

encode active m^6A demethylases that affect plant systems [16, 17]. Duan *et al.* demonstrated that the ALKBH10B-mediated demethylation of m^6A in mRNA influences the stability of mRNA for key flowering time regulators, thereby affecting flower turnover [17]. Moreover, ALKBH9B positively influences the viral abundance in plant cells. These results indicate that the extent of m^6A modifications regulated by methyltransferases and demethylases is an important factor that regulates viral infection in *A. thaliana* [16]. On the other hand, m^6A binding proteins (the readers) also play important roles in some biological processes by interacting with the m^6A modification site [18-20]. The results of the above-mentioned studies imply that the correct m^6A modification plays important regulatory roles in growth, differentiation, reproduction, and resistance to viruses [12, 14, 17].

Salt stress is one of the important environmental factors which can affect plant growth and development [21-23], such as photosynthesis [24-26], lipid metabolism [27, 28], seed germination [29, 30], signal transduction [31-33], enzyme activity [34-36], and so on. During the long evolutionary process, plants also develop many response mechanisms to salt stress [37-39], including the induce of some functional genes responsible for controlling Na^+/K^+ homeostasis, antioxidative enzyme activities [40-43], some transcription factors in response to salt stress [44-47], osmosine regulated metabolic substances such as proline [48] and plant stress hormones such as ABA [48-53]. A recent study showed that m^6A modifications were involved in the regulation of responses to salt stress in *A. thaliana*, which represents the salt-sensitive plant species [13]. There is a pressing need for defining the roles of the m^6A modification in salt-stress responses of highly salt-tolerant crop species. It will help to clarify why different plant species and even plants of the same species, but with different genotypes, have completely different salt-tolerance levels.

We speculate that the m^6A modification may be an important factor underlying these differences. Sweet sorghum [*Sorghum bicolor* (L.) Moench] is cultivated as energy [54, 55] and forage crop, in part because of its high yield and salt resistance [54, 56-58]. Therefore, sweet sorghum is highly suitable for growth on saline-alkaline land. Exploring the m^6A modification in sweet sorghum may be

pivotal for elucidating the salt-resistance mechanism of crops. Our previous studies showed that the salt-tolerant genotype M-81E has stronger salt tolerance than the salt-sensitive genotype Roma [59, 60]. Specifically, in response to a 150 mM NaCl treatment, Roma root growth was inhibited at 24 h after the salt treatment. By contrast, M-81E root growth was not inhibited until 36 h after the salt treatment [60]. These observations compelled us to use the roots of M-81E and Roma plants treated with 150 mM NaCl for 24 h as our research materials. In this study, we collected the roots of M_CK (M-81E under normal watering conditions), M_S (M-81E treated with 150 mM NaCl for 24 h), R_CK (Roma under normal watering conditions), and R_S (Roma treated with 150 mM NaCl for 24 h) for m^6A-sequencing (m^6A-seq) and mRNA-sequencing (mRNA-seq) analyses (Fig. 1a). Results delineate the m^6A modification patterns in sweet sorghum and elucidate its important regulatory effects on salt-stress responses.

2. Materials and methods

2.1. Plant materials

The M-81E and Roma sorghum genotypes were used as experimental materials. Seeds were rinsed with tap water for 8 h and then sown in pots filled with washed river sand, which was moistened with tap water. Plants were grown in a greenhouse with a 15-h light (28 °C)/9-h dark (23 °C) photoperiod and 70% relative humidity. When the plants reached the four-leaf stage, we initiated salt treatments, starting with a low concentration (50 mM NaCl) and increasing to 150 mM NaCl in 50 mM daily increments. The treatment with 150 mM NaCl lasted 24 h. Control plants were treated at the same time as the salt-treated plants, but with water instead of NaCl solutions. The roots of 2 sorghum from each treatment were mixed and stored at −70°C after quick freezing with liquid nitrogen. Two biological replicates were used for each group, resulting in a total of 8 samples.

2.2. m^{6}A-seq and RNA-seq

Total RNA was isolated and purified using TRIzol reagent (Invitrogen, Carlsbad, CA, USA) following the manufacturer's procedure. The RNA amount and purity of each sample was quantified using NanoDrop ND-1000 (NanoDrop, Wilmington, DE, USA). The RNA integrity was assessed by Bioanalyzer 2100 (Agilent, CA, USA) with RIN number >7.0, and confirmed by electrophoresis with denaturing agarose gel. Poly (A) RNA is purified from 200μg total RNA using Dynabeads Oligo (dT) 25-61005 (Thermo Fisher, CA, USA) using two rounds of purification. Then the poly (A) RNA was fragmented into small pieces using Magnesium RNA Fragmentation Module (NEB, cat.e6150, USA) under 86℃ 7min. Two libraries were constructed using cleaved RNA fragments, the input library directly following conventional RNA-seq and the IP library enriched using m^{6}A-specific antibodies (No. 202003, Synaptic Systems, Germany) incubated 2 h at 4 degrees C in IP buffers (50 mM Tris-HCl, 750 mM NaCl and 0.5% Igepal CA-630). Then the IP RNA was reverse-transcribed to create the cDNA by SuperScript™ II Reverse Transcriptase (Invitrogen, cat. 1896649, USA), which were next used to synthesize U-labeled second-stranded DNAs with E. coli DNA polymerase I (NEB, cat.m0209, USA), RNase H (NEB, cat.m0297, USA) and dUTP Solution (Thermo Fisher, cat.R0133, USA）. An A-base is then added to the blunt ends of each strand, preparing them for ligation to the indexed adapters. Each adapter contains a T-base overhang for ligating the adapter to the A-tailed fragmented DNA. Single- or dual-index adapters are ligated to the fragments, and size selection was performed with AMPureXP beads. After the heat-labile UDG enzyme (NEB, cat.m0280, USA) treatment of the U-labeled second-stranded DNAs, the ligated products are amplified with PCR by the following conditions: initial denaturation at 95℃ for 3 min; 8 cycles of denaturation at 98℃ for 15 sec, annealing at 60℃ for 15 sec, and extension at 72℃ for 30 sec; and then final extension at 72℃ for 5 min. The average insert size for the paired-end libraries was ~100 ± 50 bp. At last, libraries of RNA-seq and m^{6}A-seq performed the 2×150 bp paired-end sequencing (PE150) on an Illumina Novaseq™ 6000 (LC-Bio Technology CO., Ltd., Hangzhou, China) following the vendor's recommended protocol.

2.3. Data analysis

Fastp software (https://github.com/OpenGene/fastp) was used to remove the reads that contained adaptor contamination, low-quality bases, and undetermined bases with default parameters. Then sequence quality of IP and Input samples were also verified using fastp. We used HISAT2 [61] (http://daehwankimlab.github.io/hisat2) to map reads to the reference genome (Sorghum_bicolor_NCBIv3, ftp://ftp.ensemblgenomes.org/pub/plants/release-48/fasta/sorghum_bicolor/). Mapped reads of IP and input libraries were provided for R package exomePeak [62] (https://bioconductor.org/packages/exomePeak), FDR＜0.05, which identifies m^6A peaks with the bed or bigwig format that can be adapted for visualization on the IGV software (http://www.igv.org). HOMER (http://homer.ucsd.edu/homer/motif) was used for de novo motif finding followed by localization of the motif with respect to peak summit. Called peaks were annotated by intersection with gene architecture using R package ChIPseeker [63] (https://bioconductor.org/packages/ChIPseeker). Then StringTie [64] (https://ccb.jhu.edu/software/stringtie) was used to perform expression level for all mRNAs from input libraries by calculating FPKM (total exon fragments /mapped reads (millions) × exon length (kB)). The differentially expressed mRNAs were selected with log2 (fold change) >1 or log2 (fold change) <-1 and p value < 0.05 by R package edgeR [65] (https://bioconductor.org/packages/edgeR). The raw sequence data has been uploaded to NCBI under accession number GSE146936 (https://www.ncbi.nlm.nih.gov/geo/query/acc.cgi?acc=GSE146936).

2.4. Quantitative real-time PCR analysis

The same materials as mRNA-seq and m^6A-seq extracted total RNA was used for the qRT-PCR. The qRT-PCR analyses were carried out using AceQ Universal SYBR qPCR Master Mix (Vazyme Biotech Co., Ltd) on a Bio-Rad CFX96 Real-Time Detection System. The relative expression level of *SbMTA*, *SbMTB*, *SbMTC*, *SbFIP37*, and ALKBH family genes was detected by quantitative real-time

PCR (qRT-PCR). *S. bicolor*'s β-actin (Gene ID: SORBI_3001G112600) was used as an internal standard, Cq mean=26.84. Three biological replicates were analyzed for each gene. Primer sequences are listed in Table S1. The measurement and calculation were performed as described previously [66, 67].

2.5. Transcript stability time course

When sweet sorghum grows to the four-leaf stage, salt treatment is carried out, and the treatment method is the same as in "2.1". When the final salt concentration is reached and treated for 0 h and 24 h, continue to treat 0h and 24h with 1/2 Hoagland solution containing 10 μM actinomycin D and 0.6 mM cordycepin. Total RNA was extracted and reverse transcribed using oligo dT primers. Primer sequences are listed in Table S1. The measurement and calculation were performed as described previously [66, 67].

2.6. GO and KEGG analysis

The amount of gene expression was expressed in reads per thousand base pairs per million mapped reads, and we used the DESeq protocol to identify differentially expressed genes (DEGs) [68]. Gene annotation and classification were performed as described previously [59].

Gene ontology (GO) annotations of unigenes were made using the Blast2GO program [69], and then GO functional classification was performed using WEGO software [70]. The GO terms shown are significantly enriched, and to answer the biological functions of these m^6A modifications, we have displayed more GO terms related to the biological process in limited pictures rather than cellular component and molecular function. The Clusters of Orthologous Groups of proteins (COG) functional annotation of unigenes was performed using the COG online comparison program [71]. Using the Kyoto Encyclopedia of Genes and Genomes (KEGG) database [72], unigenes were annotated to different metabolic pathways to identify their unique functions.

3. Results

3.1. Quality and depth of RNA sequencing

To identify the roles of the m^6A modification on the salt-resistance in sweet sorghum, we completed the m^6A RNA immunoprecipitation and sequencing (m^6A-seq) analysis with poly-A^+ RNA (IP) of samples, whereas the RNA-seq analysis involved poly-A^+ RNA without RIP (as the control for m^6A-seq), with two replicates for each sample. A total of 25-64 million reads were generated for each m^6A-seq sample and 37-61 million reads for each mRNA-seq sample. The proportion of cleanly mapped reads and transcripts for m^6A-seq was approximately 70–84%, with a Q30 greater than 94% for each sample (Table S2). These results reflected the high quality and depth of the generated m^6A-seq data.

3.2. Characteristics and extent of the m^6A modification in sweet sorghum roots

We identified 10,194 m^6A peaks representing the transcripts of 8,116 genes in M_CK, and 5,946 m^6A peaks representing the transcripts of 5,218 genes in R_CK (Fig. 1b; Table S3). A total of 6,039 and 1,791 m^6A peaks were exclusively detected in M_CK and R_CK, respectively. Moreover, 4,155 peaks were detected for both M_CK and R_CK (Fig. 1c). We speculated that the common peaks in M_CK and R_CK may represent the conserved m^6A modifications among diverse sweet sorghum genotypes, which might be crucial for normal growth and development. To further reveal the functions of these conserved m^6A modifications, we selected genes corresponding to the common m^6A peaks in M_CK and R_CK for a gene ontology (GO) analysis (Fig. 1d). Our result shows that the common m^6A peaks were highly enriched among these genes in GO terms: regulation of transcription, oxidation-reduction process, response to cadmium ion transcription, response to salt stress, glycolytic process, protein phosphorylation, translation, response to cold, response to abscisic acid, embryo development ending in seed dormancy, protein folding, intracellular protein transport, and response to water deprivation. Many of

these biological processes are related to growth, development, and responses to environmental stresses, which may reflect specific root activities in response to the surrounding complex soil environment. Interestingly, the m^{6}A peaks were highly enriched with the transcripts of embryonic development-related genes, suggesting that m^{6}A modifications are required for embryonic development in mammals and plants [12, 73].

3.3. Relationship between m^{6}A modification positions and transcription in sweet sorghum

The consensus m^{6}A modification sequence has been revealed as 'RRm^{6}ACH' (where R is A/G and H is A/C/U) [3, 4]. Our m^{6}A-seq data for sweet sorghum indicated that more than 50% of the RIP fragments contained this consensus sequence (Fig. 2a). To further characterize the m^{6}A in the transcripts of sweet sorghum, we investigated the metagene profiles of the m^{6}A peaks. Consistent with the distribution of reads, the m^{6}A peaks for M-81E were abundant in regions near the 3' untranslated region (UTR) after the stop codon (71%), in the coding sequence (CDS) (18%), and in the 5' UTR before the start codon (11%). In Roma, the m^{6}A peaks were abundant in regions near the 3' UTR after the stop codon (80%), in the CDS (13%), and in the 5' UTR before the start codon (8%) (Fig. 2b; Fig. S1; Table S3). A transcriptome-wide analysis revealed a similarity in the regions with m^{6}A modifications in M-81E and Roma. Additionally, the observed m^{6}A modification patterns were similar to those reported in *A. thaliana* and rice [2, 3, 13], implying the m^{6}A modified regions may be conserved among various plant species. To examine the differences in the prominent m^{6}A peaks between genotypes, we analyzed the top 1,000 most significant peaks in M-81E and Roma (Fig. 2c). We detected more significant m^{6}A peaks concentrated in the 5' UTR in M-81E than in Roma. To assess the effects of the diversity in the m^{6}A-modified regions on the mRNA in sweet sorghum, we further analyzed the mRNA levels following the m^{6}A modification of specific regions. The m^{6}A modifications in the 5' UTR region resulted in the highest

mRNA levels, followed by the modifications of the 3' UTR and then the modifications of the CDS region (Fig. 2d). The differential expression of genes in plants of different genotypes or varieties is one of the major factors contributing to the variability in plant salt tolerance [74, 75]. Our results suggested that differences in the regions with significant m^6A peaks may be responsible for the differential gene expression of M-81E and Roma. In mammals, heat-shock stress enhances the m^6A modifications in the 5' UTR, which then promotes cap-independent translation [10]. The greater m^6A modification of the 5' UTR region in M-81E than in Roma may be associated with increased transcription and translation in M-81E.

3.4. The M-81E roots undergo few salt stress-induced changes to m^6A modifications

We used exomePeak to process the data and obtain information regarding the m^6A peaks for salt-stressed M-81E and Roma plants. We identified 10,241 m^6A peaks representing the transcripts of 8,181 genes expressed in the M_S roots (Fig. 3a). There were relatively few changes to the m^6A modifications of M-81E in response to the salt treatment. We subsequently compared the m^6A modifications in M_CK and M_S root samples. Our data indicated that 80.9% of the m^6A peaks overlapped between the M_S and M_CK samples. To explore the relationship between m^6A peaks changes and gene expression changes, we compared genes with significant differences in m^6A peaks and mRNA abundance (Fig. 3b, 3c). This result suggested that there was less overlap between m^6A peak changes and gene expression changes, the regulation of m^6A modification on RNA fate is complicated, rather than simply promoting or decreasing mRNA abundance within the transcriptome. KEGG analysis of differential m^6A peaks genes revealed that differential m^6A peak was mainly focused on genes related to basic cellular metabolisms, such as phenylpropanoid biosynthesis, purine metabolism, and pyrimidine metabolism. DEGs mainly focus on genes related to plant hormone signal transduction (Fig. 3d).

Although the effect of m^6A modification on the fate of mRNA is unknown, the biological function of m^6A modification depends on the function of the modified gene itself. Analysis of the dynamic mapping of m^6A modification under salt stress can help us understand the biological functions involved in m^6A modification under salt stress. We compared the m^6A-modified genes in M_CK and M_S regarding GO annotations (Fig. 3e, Table S5). Our results indicated there were relatively few differences in the m^6A modifications and gene expression between M_CK and M_S. This observation is consistent with the physiological data generated in our previous study that revealed M-81E is not considerably affected by a 24-h treatment with 150 mM NaCl [60]. These results implied that the m^6A modifications in M-81E due to 24-h exposure to 150 mM NaCl can maintain the salt tolerance of this genotype. Consequently, comparisons with M-81E may be relevant for investigating the dynamic changes to the salt-induced m^6A modifications in the salt-sensitive genotype Roma, and may be useful for clarifying the possible biological effects of the changes in the m^6A modifications in Roma.

3.5 The Roma roots undergo major salt stress-induced changes to m^6A modifications

In contrast to the data for M-81E, we identified 12,046 m^6A peaks representing the transcripts of 9,820 genes expressed in the salt-sensitive R_S roots (Fig. 4a). Moreover, there were near twice as many m^6A modifications in R_S than in R_CK. In addition to the 6,336 m^6A peaks that were common to both R_S and R_CK samples, 5,489 m^6A peaks specific for R_S samples were identified after salt treatment. In other words, the m^6A modification and gene expression patterns induced by salt stress varied considerably between M-81E and Roma, with greater changes to m^6A modifications and gene expression in Roma (Fig. 4b, 4c).

And the m^6A modification changes are more drastic than the gene expression changes. This means that relative to gene expression, m^6A modification changes seem to be more sensitive and intense in the process of regulating salt tolerance in

Roma. We compared genes with significant differences in m^6A peaks and mRNA abundance. KEGG analysis revealed that differential m^6A peak was mainly focused on genes related to starch and sucrose metabolism, peroxisome, and nucleotide excision repair (Fig. S2). DEGs were mainly focused on genes related to starch and sucrose metabolism, amino sugar and nucleotide sugar metabolism, oxidative phosphorylation, and glycolysis/gluconeogenesis.

Besides, we selected genes associated with m^6A modifications in Roma under salt stress and control conditions for a GO analysis (Fig. 4d). The following GO terms were highly enriched among these genes: regulation of transcription, oxidation-reduction process, protein phosphorylation, defense response, carbohydrate metabolic process, and response to salt stress. These results are similar to those of a previous *A. thaliana* study that confirmed that salt-related transcripts undergo m^6A modifications in response to salt stress [13]. Accordingly, the changes to the m^6A modifications in Roma may positively affect salt-stress responses. In particular, changes in the m^6A modification of some key salt-tolerant genes may play a more important role.

3.5 m^6A modification regulates mRNA abundance by regulating the stability of salt-tolerant transcripts

When we analyzed the transcripts with significant changes in m6A modification in Roma, we found an interesting phenomenon: some transcripts of salt-tolerance-related genes with significantly increased m^6A modification have a significant increase in mRNA abundance at the same time (Table1). For example, in our m^6A-IP data, we observed significant m^6A change around the stop codon of *SbIAR4* (SORBI_3010G101300) and *SbNRT1.5* (SORBI_3004G276200) in Roma (Fig. 5a), and the mRNA abundance increased significantly. *IAR4* is a key gene that regulates root hair formation and root development [76, 77]. *NRT1.5* is a proton-coupled H^+/K^+ antiporter, which plays a vital role in the K^+ transport from root to stem and also participates in the regulation of K^+/NO_3^- distribution in plants

[78, 79].

To explore whether m^6A regulates RNA abundance by affecting the stability of mRNA, we treated R_CK and R_S with transcription inhibitors cordycepin and actinomycin D for 0 h and 24 h. We then calculated the percentage of initial transcripts remaining 24 h after treatment using qRT-PCR. Studies on mRNA stability have shown that the m^6A modification on these key salt-tolerant transcripts increases mRNA stability, resulting increase in mRNA abundance (Fig. 5b).

3.6. Potential consequences of the differences in m^6A modifications between M-81E and Roma

To explore the potential effects of the differences in the m^6A modifications between M_CK and R_CK, we compared the differentially expressed genes and the differentially m^6A peak between M_CK and R_CK (Fig. 6a, 6b; Table S5). The M-81E and Roma genotypes differed more in terms of m^6A modifications than regarding gene expression, suggesting that the differential of m^6A modification may play a more important role in maintaining the differential salt tolerance between M-81E and Roma, relative to the differential gene expression.

To explore the function of m^6A modification of M-81E and Roma under salt stress. we performed GO analysis of the genes corresponding to the m^6A-modified genes in M_CK, M_S, R_CK, and R_S (Fig. 6c, Table S4). In salt-resistant genotype M-81E, there was little change in of m^6A modification under salt stress. However, in salt-sensitive genotype Roma, the m^6A modification was changed greatly, and the m^6A modification in R_S was similar to M-81E. Compared with the R_CK, most of the M_CK, M_S, and R_S genes were annotated with GO terms from the cellular component, molecular function, and biological process categories. Specifically, the highly enriched biological process GO terms were the regulation of transcription, DNA-templated; transcription, DNA-templated; protein phosphorylation; oxidation-reduction process; defense response; response to abscisic acid; response to salt stress.

This result suggested that the m^{6}A-modified genes that play a positive role in maintaining salt tolerance in different genotypes of sweet sorghum appear to be fixed. Next, we compared genes with significant differences in m^{6}A peaks and mRNA abundance in M_CK and R_CK (Fig. 6d). KEGG analysis revealed that differential m^{6}A peak was mainly focused on genes related to oxidative phosphorylation, starch and sucrose metabolism. DEGs were mainly focused on genes related to plant-pathogen interaction, phenylpropanoid biosynthesis, and amino sugar and nucleotide sugar metabolism. These m^{6}A-modified genes may be able to precisely and effectively mitigate the adverse consequences of salt, osmotic, and oxidative stresses, and contribute to the differences in the salt tolerance of M-81E and Roma.

3.7. Methylase and demethylase activities in sweet sorghum

The extent of the m^{6}A modifications in eukaryotes is mainly regulated by methylases and demethylases. The m^{6}A-seq results of Anderson et al. revealed that the *A. thaliana mta* mutant has considerably fewer m^{6}A modifications than the wild-type controls [13]. We identified the major sweet sorghum methylase genes *SbMTA*, *SbMTB*, *SbFIP37*, and *SbMTC* as well as the main ALKBH demethylase family members via a BLAST search (Table S5). We also verified the salt stress-induced changes to the expression of these genes in a quantitative real-time PCR assay. There were no significant changes in the expression levels of the methylase and demethylase genes in M-81E under saline conditions. In contrast, the expression of the main methylase gene (*SbMTA*) was upregulated by salt stress in Roma, whereas the expression of the ALKBH demethylase gene family was downregulated (Fig. S3). This result is consistent with the gene expression trend in mRNA-seq. The changes in the expression levels of the major methylase and demethylase genes in sweet sorghum roots implied that salt stress does not affect the m^{6}A modifications in M-81E, whereas it generally increases the m^{6}A modifications in Roma. These observations were consistent with the changes in the number and extent of the m^{6}A peaks revealed in our m^{6}A-seq analysis.

4. Discussion

4.1 The m^{6}A modifications in roots are mainly enriched in transcripts related to environmental changes

The m^{6}A modification is the most important post-transcriptional regulatory factor determining the translation of mRNA. For example, in *A. thaliana*, a decrease in the m^{6}A modification of the key genes *STM* and *WUS* in the shoot apical meristem leads to abnormal stem cell development [14]. In *A. thaliana*, the excessive m^{6}A modification of *SPL3* and *SPL9* adversely affects the expression of the flowering activation gene *FT*, resulting in delayed flowering [17]. Moreover, a transcriptome-wide analysis of the m^{6}A modifications in *A. thaliana* revealed differences in the m^{6}A modifications between ecotypes and between plant organs [2, 4]. For example, the leaf-specific m^{6}A modified transcripts are mainly enriched in genes related to photosynthesis and respiratory metabolism, while the transcripts in roots are mainly enriched in genes that respond to stress, redox processes, and transporters. However, a large number of m^{6}A modified transcripts in flowers are related to reproductive development, stress response, cell proliferation and differentiation [4]. Studies in different tissues of rice also showed that specific m^{6}A in callus is mainly enriched in transcripts related to basic metabolisms such as cell growth and division [3]. The specific m^{6}A modification in leaves is mainly enriched in transcripts related to photosynthesis. These observations suggest that the transcripts modified by m^{6}A usually depend on the specific functions of the tissues or organs. And the GO annotation of m^{6}A modified transcripts can partially explain the biological significance of m^{6}A modification.

Among the various plant organs, the roots are likely exposed to the most complex and diverse environments. Additionally, the roots are the first organs directly exposed to salt stress. Our results suggest that m^{6}A modification in roots is primarily related to genes associated with growth and response to environmental stress (Fig. 1d), which may be related to the specific biological function of roots

requiring a timely response to complex environments. The m^6A modification pattern in sorghum is similar to that reported in other plants [2-4, 13, 80, 81], which may mean that m^6A modification is conservative in different plants. Therefore, analyzing the m^6A modification patterns in salt-stressed roots is an effective way to characterize the mechanism regulating salt tolerance at the post-transcriptional level.

Our result shows that there was less overlap between m^6A peak changes and gene expression changes in different groups. This means that the function of m^6A modification on RNA fate is complicated, and only a very few m^6A modifications on genes directly regulate mRNA abundance. Most of the m^6A modifications may play a regulatory role by influencing other RNA metabolic processes. Functional annotation of m^6A modified genes can help us understand the biological functions involved in m^6A modifications that change significantly under salt stress.

4.2 m^6A modification regulates salt resistance in sweet sorghum by regulating mRNA stability of key transcripts under salt stress

A recent study showed that exposure to salt stress increases the extent of m^6A modifications in *A. thaliana*, and upregulates the expression of salt-responsive genes [13], confirming that the m^6A modification of salt stress-related transcripts is closely related to the regulation of plant responses to salt stress.

Similar results were also observed in our study: The m^6A modification can improve the mRNA stability of some key salt-tolerant gene transcripts, thereby increasing mRNA abundance (such as *AVP1* and *IAR4*). These key genes for salt resistance play an active role in regulating plant response to salt stress. In Arabidopsis, overexpression of *AVP1* leads to increased ion uptake by vacuoles in plants. Under high Na^+ concentration, the increase of H^+ concentration can also enhance the driving force of AtNHX1 mediated Na^+/ H^+ exchange, thereby helping to chelate Na^+ into the vacuoles of plants [82]. At the same time, the increase in the expression level of *AVP1* leads to an increase in the solute content in the vacuole, which makes the cells have strong water retention, and thus their tolerance to salt

and drought stress was enhanced. The *IAR4* mutant *iar4* has increased sensitivity to salt stress conditions and has a low survival rate. At the same time, more Na^+ and ROS are accumulated in *iar4*, which indicates that *IAR4* plays an active role in regulating salt stress [77].

Although only a few key salt-tolerant transcripts can be accurately detected at present, the m^6A modification directly regulates mRNA abundance. However, it can be speculated that more m^6A modifications on key salt-tolerant transcripts will provide more complex and sophisticated salt stress regulation pathways, such as RNA splicing, RNA export, 3′ UTR processing, and translation, leading to higher salt tolerance in plants.

4.3 The regulatory effect of m^6A modification on salt stress was limited by the initial m^6A

In the current study, the extent of the m^6A modifications and gene expression was similar between M_CK and M_S root samples. This result contradicts the findings of an earlier investigation involving *A. thaliana*, but is similar to the results of one of our previous studies in which a 24 h treatment with 150 mM NaCl did not affect M-81E root growth [60]. This observation may be explained by the fact that the m^6A modifications in M_CK roots are enough to mitigate the damage caused by a 24 h treatment with 150 mM NaCl.

In the salt-sensitive genotype Roma, m^6A modification changed drastically under salt stress. The genes corresponding to the transcripts regulated by m^6A modifications are highly enriched on genes related to the regulation of transcription, oxidation-reduction process, protein phosphorylation, defense response, carbohydrate metabolic process, and response to salt stress. It is well known that salt stress damages plant mainly through ion stress and osmotic stress. In plant cells, proline, soluble sugar, and soluble protein are three common organic osmotic adjustment substances. Ashraf et al.'s research on salt-tolerant *Eruca sativa* and salt-sensitive *Eruca sativa* found that the concentration of soluble sugar in the leaves

of salt-resistant *Eruca sativa* was significantly higher than that of salt-sensitive *Eruca sativa* [83]. Feng et al. observed similar results in corn roots. Higher soluble sugar and electrolyte concentration can give corn a higher osmotic adjustment ability [84]. Therefore, we speculate that more m^6A modifications on starch and sugar metabolism-related genes in R_S may lead to more accumulation of osmotic adjustment substances, which leads to relatively high salt tolerance. Similarly, the m^6A modification on the gene transcripts of the oxidative phosphorylation pathway may alleviate the oxidative stress caused by salt stress. This change in m^6A modifications positively regulates plant salt tolerance [13]. However, this response does not completely alter the salt tolerance of plants. The growth of both *A. thaliana* and Roma plants is severely inhibited by salt stress [13, 60]. This is in contrast to the phenotype of the salt-tolerant M-81E. Thus, we suggest that the increase in m^6A modifications in salt-treated Roma is likely a compensatory response to the salt stress. Additionally, m^6A is relatively abundant in the salt-responsive transcripts of M-81E, even in the absence of salinity stress. For plant salt tolerance, the regulation of salt-tolerant genes is a quantitative trait, rather than relying on a certain gene or genes to play a decisive role. Therefore, more m^6A modifications on salt-tolerant transcripts may provide more control methods under salt stress. Our result suggested that m^6A modifications are indispensable for the regulation of salt stress responses. However, there are some limitations to this regulatory activity, which does not fundamentally change the salt tolerance of sweet sorghum. The regulatory strength may depend on its own initial m^6A modification level.

Recent studies have indicated that different stimuli (including heat shock, sodium arsenite, and endoplasmic reticulum stress) in mammals lead to the relocating of m^6A binding protein YTHDF-mediated mRNA in the cytoplasm and affect the translation process (translation efficiency) [85]. In plants, heat stress also causes the relocating of the YTHDF homolog ECT2 in the cytoplasm [18-20]. This suggests that there may be similar regulatory patterns in plants as in mammals. Under stress conditions, the distribution of m^6A-mRNA to different parts of cells by ECT-m^6A-mRNA complex may endow m^6A-mRNA with different fates. For this

reaction is very rapid, we speculate that the biological process may depend on the Ca^{2+} transport pathway. Previous studies have shown that members of the ECT family can interact with the calcineurin B-like-interacting protein kinase family (CIPK) [86]. For example, ECT1/ECT2 can interact with CIPK1, ECT11 can interact with CIPK3. The CBL-CIPK calcium signaling pathway is one of the main calcium signaling pathways in plants. It plays an important role in regulating plant responses to cold, drought, salinity, and abscisic acid stimulation [87, 88]. Co-transformation experiments show that the localization of ECT1 in cells is regulated by Ca^{2+} signaling pathway [86]. This regulation process mainly depends on the m^6A modification of the mRNA before stress, rather than the newly generated m^6A modification [18-20, 85].

In M-81E and Roma, the differences in the m^6A modifications are much greater than the differences in gene expression levels and are more sensitive. After salt treatment, the change of m^6A modification level also appeared to be more drastic than the change of gene expression. m^6A modifications showed stronger sensitivity than direct transcriptional regulation in regulating salt tolerance. This evidence combined with our research suggested that the number and extent of the initial m^6A modifications on the transcripts of salt-resistance genes may be used as a new reference for evaluating crop salt tolerance.

5. Conclusions

In-depth m^6A sequencing analysis revealed that there are considerable differences in the m^6A modifications of M-81E and Roma. These differences may be physiologically related to the observed variations in the salt tolerance of plant species. m^6A modification regulates mRNA abundance by regulating the stability of salt-tolerant transcripts, and the regulatory activity is limited by the initial m^6A modification level. Our results suggested that the number and extent of m^6A modifications on the salt-resistance-related mRNA may be important parameters in assessing the salt tolerance of crops.

Conflict of interest

The authors declare that they have no conflicts of interest.

Acknowledgements

We are grateful for financial support from the National Natural Science Research Foundation of China (31871538, U1906204), the National Key R&D Program of China (2018YFD1000700, 2018YFD1000704), Shandong Province Key Research and Development Program (2019GSF107079), the Development Plan for Youth Innovation Team of Shandong Provincial (2019KJE012), the Opening Foundation of Shandong Key Laboratory of Crop Genetic Improvement, Ecology and Physiology (SDKL2018008-3), the Royal Society University Research Fellowship (UF120411 and URF\R\180030, L.-N.L.), the Royal Society Fellow Enhancement Awards (RGF\EA\181061 and RGF\EA\180233, L.-N.L.), and Biotechnology and Biological Sciences Research Council Grant (BB/M024202/1 and BB/R003890/1, L.-N.L.).

Author Contributions

Hongxiang Zheng, Xi Sun, Luning Liu, and Na Sui prepared the manuscript. Hongxiang Zheng, Jinlu Li, Yushuang Song, and Jie Song performed some experiments; Hongxiang Zheng, Xiansheng Zhang, and Na Sui collected data and carried out all analyses; Na Sui and Xiansheng Zhang conceptualized the idea and revised the manuscript. All authors read and approved the final manuscript.

References

[1] D. Dominissini, S. Moshitch-Moshkovitz, S. Schwartz, M. Salmon-Divon, L. Ungar, S. Osenberg, K. Cesarkas, J. Jacob-Hirsch, N. Amariglio, M. Kupiec, R. Sorek, G. Rechavi, Topology of the human and mouse m^6A RNA methylomes revealed by m^6A-seq, Nature, 485 (2012) 201.

[2] G.-Z. Luo, A. MacQueen, G. Zheng, H. Duan, L.C. Dore, Z. Lu, J. Liu, K. Chen, G. Jia, J. Bergelson, C. He, Unique features of the m^6A methylome in *Arabidopsis thaliana*, Nature Communications, 5 (2014) 5630.

[3] Y. Li, X. Wang, C. Li, S. Hu, J. Yu, S. Song, Transcriptome-wide N^6-methyladenosine profiling of rice callus and leaf reveals the presence of tissue-specific competitors involved in selective mRNA modification, RNA biology, 11 (2014) 1180-1188.

[4] Y. Wan, K. Tang, D. Zhang, S. Xie, X. Zhu, Z. Wang, Z. Lang, Transcriptome-wide high-throughput deep m^6A-seq reveals unique differential m^6A methylation patterns between three organs in *Arabidopsis thaliana*, Genome Biology, 16 (2015) 272.

[5] J.A. Bokar, M.E. Rath-Shambaugh, R. Ludwiczak, P. Narayan, F. Rottman, Characterization and partial purification of mRNA N^6-adenosine methyltransferase from HeLa cell nuclei. Internal mRNA methylation requires a multisubunit complex, Journal of Biological Chemistry, 269 (1994) 17697-17704.

[6] S.D. Agarwala, H.G. Blitzblau, A. Hochwagen, G.R. Fink, RNA methylation by the MIS complex regulates a cell fate decision in yeast, PLoS genetics, 8 (2012) e1002732.

[7] J. Liu, Y. Yue, D. Han, X. Wang, Y. Fu, L. Zhang, G. Jia, M. Yu, Z. Lu, X. Deng, A METTL3–METTL14 complex mediates mammalian nuclear RNA N^6-adenosine methylation, Nature chemical biology, 10 (2014) 93.

[8] G. Jia, Y. Fu, X. Zhao, Q. Dai, G. Zheng, Y. Yang, C. Yi, T. Lindahl, T. Pan, Y.-G. Yang, N^6-methyladenosine in nuclear RNA is a major substrate of the

obesity-associated FTO, Nature chemical biology, 7 (2011) 885.

[9] G. Zheng, J.A. Dahl, Y. Niu, P. Fedorcsak, C.-M. Huang, C.J. Li, C.B. Vågbø, Y. Shi, W.-L. Wang, S.-H. Song, ALKBH5 is a mammalian RNA demethylase that impacts RNA metabolism and mouse fertility, Molecular cell, 49 (2013) 18-29.

[10] Kate D. Meyer, Deepak P. Patil, J. Zhou, A. Zinoviev, Maxim A. Skabkin, O. Elemento, Tatyana V. Pestova, S.-B. Qian, Samie R. Jaffrey, 5′ UTR m^6A promotes cap-independent translation, Cell, 163 (2015) 999-1010.

[11] H. Zheng, S. Li, X.S. Zhang, N. Sui, Functional implications of active N 6-methyladenosine in plants, Frontiers in Cell and Developmental Biology, 8 (2020) 291.

[12] S. Zhong, H. Li, Z. Bodi, J. Button, L. Vespa, M. Herzog, R.G. Fray, MTA is an *Arabidopsis* messenger RNA adenosine methylase and interacts with a homolog of a sex-specific splicing factor, The Plant Cell, 20 (2008) 1278-1288.

[13] S.J. Anderson, M.C. Kramer, S.J. Gosai, X. Yu, L.E. Vandivier, A.D.L. Nelson, Z.D. Anderson, M.A. Beilstein, R.G. Fray, E. Lyons, B.D. Gregory, N^6-methyladenosine inhibits local ribonucleolytic cleavage to stabilize mRNAs in *Arabidopsis*, Cell Reports, 25 (2018) 1146-1157.e1143.

[14] L. Shen, Z. Liang, X. Gu, Y. Chen, Zhi Wei N. Teo, X. Hou, Weiling M. Cai, Peter C. Dedon, L. Liu, H. Yu, N^6-methyladenosine RNA modification regulates shoot stem cell fate in *Arabidopsis*, Developmental Cell, 38 (2016) 186-200.

[15] K. Růžička, M. Zhang, A. Campilho, Z. Bodi, M. Kashif, M. Saleh, D. Eeckhout, S. El- Showk, H. Li, S. Zhong, Identification of factors required for m^6A mRNA methylation in *Arabidopsis* reveals a role for the conserved E3 ubiquitin ligase HAKAI, New Phytologist, 215 (2017) 157-172.

[16] M. Martínez-Pérez, F. Aparicio, M.P. López-Gresa, J.M. Bellés, J.A. Sánchez-Navarro, V. Pallás, *Arabidopsis* m^6A demethylase activity modulates viral infection of a plant virus and the m^6A abundance in its genomic RNAs, Proceedings of the National Academy of Sciences, 114 (2017) 10755.

[17] H.-C. Duan, L.-H. Wei, C. Zhang, Y. Wang, L. Chen, Z. Lu, P.R. Chen, C. He, G. Jia, ALKBH10B is an RNA N^6-methyladenosine demethylase affecting Arabidopsis

floral transition, The Plant Cell, 29 (2017) 2995.

[18] L.-H. Wei, P. Song, Y. Wang, Z. Lu, Q. Tang, Q. Yu, Y. Xiao, X. Zhang, H.-C. Duan, G. Jia, The m^6A Reader ECT2 controls trichome morphology by affecting mRNA stability in *Arabidopsis*, The Plant Cell, 30 (2018) 968.

[19] J. Scutenaire, J.-M. Deragon, V. Jean, M. Benhamed, C. Raynaud, J.-J. Favory, R. Merret, C. Bousquet-Antonelli, The YTH domain protein ECT2 is an m^6A Reader required for normal trichome branching in *Arabidopsis*, The Plant Cell, 30 (2018) 986.

[20] L. Arribas-Hernández, S. Bressendorff, M.H. Hansen, C. Poulsen, S. Erdmann, P. Brodersen, An m^6A-YTH module controls developmental timing and morphogenesis in *Arabidopsis*, The Plant Cell, 30 (2018) 952.

[21] Y. Deng, Z. Feng, F. Yuan, J. Guo, S. Suo, B. Wang, Identification and functional analysis of the autofluorescent substance in Limonium bicolor salt glands, Plant physiology and biochemistry, 97 (2015) 20-27.

[22] J. Song, B. Wang, Using euhalophytes to understand salt tolerance and to develop saline agriculture: Suaeda salsa as a promising model, Annals of Botany, 115 (2015) 541-553.

[23] F. Yuan, B. Leng, B. Wang, Progress in studying salt secretion from the salt glands in recretohalophytes: how do plants secrete salt?, Frontiers in plant science, 7 (2016) 977.

[24] K. Li, C.-H. Pang, F. Ding, N. Sui, Z.-T. Feng, B.-S. Wang, Overexpression of Suaeda salsa stroma ascorbate peroxidase in Arabidopsis chloroplasts enhances salt tolerance of plants, South African Journal of Botany, 78 (2012) 235-245.

[25] Z. Feng, Y. Deng, H. Fan, Q. Sun, N. Sui, B. Wang, Effects of NaCl stress on the growth and photosynthetic characteristics of Ulmus pumila L. seedlings in sand culture, Photosynthetica, 52 (2014) 313-320.

[26] L.-Q. Qin, L. Li, C. Bi, Y.-L. Zhang, S.-B. Wan, J.-J. Meng, Q.-W. Meng, X.-G. Li, Damaging mechanisms of chilling-and salt stress to Arachis hypogaea L. leaves, Photosynthetica, 49 (2011) 37-42.

[27] N. Sui, G. Han, Salt-induced photoinhibition of PSII is alleviated in halophyte

Thellungiella halophila by increases of unsaturated fatty acids in membrane lipids, Acta Physiologiae Plantarum, 36 (2014) 983-992.

[28] N. Sui, Y. Wang, S. Liu, Z. Yang, F. Wang, S. Wan, Transcriptomic and physiological evidence for the relationship between unsaturated fatty acid and salt stress in peanut, Frontiers in plant science, 9 (2018) 7.

[29] Y. Guo, W. Jia, J. Song, D. Wang, M. Chen, B. Wang, Thellungilla halophila is more adaptive to salinity than Arabidopsis thaliana at stages of seed germination and seedling establishment, Acta Physiologiae Plantarum, 34 (2012) 1287-1294.

[30] J. Song, J. Zhou, W. Zhao, H. Xu, F. Wang, Y. Xu, L. Wang, C. Tian, Effects of salinity and nitrate on production and germination of dimorphic seeds applied both through the mother plant and exogenously during germination in S uaeda salsa, Plant species biology, 31 (2016) 19-28.

[31] M. Li, S. Guo, Y. Xu, Q. Meng, G. Li, X. Yang, Glycine betaine- mediated potentiation of HSP gene expression involves calcium signaling pathways in tobacco exposed to NaCl stress, Physiologia plantarum, 150 (2014) 63-75.

[32] T. Su, W. Li, P. Wang, C. Ma, Dynamics of peroxisome homeostasis and its role in stress response and signaling in plants, Frontiers in Plant Science, 10 (2019) 705.

[33] J. Guo, C. Lu, F. Zhao, S. Gao, B. Wang, Improved reproductive growth of euhalophyte Suaeda salsa under salinity is correlated with altered phytohormone biosynthesis and signal transduction, Functional Plant Biology, 47 (2020) 170-183.

[34] X. Kong, J. Pan, M. Zhang, X. Xing, Y. Zhou, Y. Liu, D. Li, D. Li, ZmMKK4, a novel group C mitogen- activated protein kinase kinase in maize (Zea mays), confers salt and cold tolerance in transgenic Arabidopsis, Plant, cell & environment, 34 (2011) 1291-1303.

[35] L. Zhang, Y. Li, W. Lu, F. Meng, C.-a. Wu, X. Guo, Cotton GhMKK5 affects disease resistance, induces HR-like cell death, and reduces the tolerance to salt and drought stress in transgenic Nicotiana benthamiana, Journal of experimental botany, 63 (2012) 3935-3951.

[36] D. Zhang, S. Jiang, J. Pan, X. Kong, Y. Zhou, Y. Liu, D. Li, The overexpression of a maize mitogen- activated protein kinase gene (Z m MPK 5) confers salt stress

tolerance and induces defence responses in tobacco, Plant biology, 16 (2014) 558-570.
[37] X. Sun, G. Han, Z. Meng, L. Lin, N. Sui, Roles of malic enzymes in plant development and stress responses, Plant signaling & behavior, 14 (2019) e1644596.
[38] X. Wang, X. Chen, Q. Wang, M. Chen, X. Liu, D. Gao, D. Li, L. Li, MdBZR1 and MdBZR1-2like Transcription Factors Improves Salt Tolerance by Regulating Gibberellin Biosynthesis in Apple, Frontiers in Plant Science, 10 (2019) 1473.
[39] F. Jia, C. Wang, J. Huang, G. Yang, C. Wu, C. Zheng, SCF E3 ligase PP2-B11 plays a positive role in response to salt stress in Arabidopsis, Journal of experimental botany, 66 (2015) 4683-4697.
[40] D.G. Hu, Q.J. Ma, C.H. Sun, M.H. Sun, C.X. You, Y.J. Hao, Overexpression of MdSOS2L1, a CIPK protein kinase, increases the antioxidant metabolites to enhance salt tolerance in apple and tomato, Physiologia plantarum, 156 (2016) 201-214.
[41] Y. Chen, Y. Han, X. Kong, H. Kang, Y. Ren, W. Wang, Ectopic expression of wheat expansin gene TaEXPA2 improved the salt tolerance of transgenic tobacco by regulating Na+/K+ and antioxidant competence, Physiologia plantarum, 159 (2017) 161-177.
[42] M. Zhang, G.-Q. Zhang, H.-H. Kang, S.-M. Zhou, W. Wang, TaPUB1, a putative E3 ligase gene from wheat, enhances salt stress tolerance in transgenic Nicotiana benthamiana, Plant and Cell Physiology, 58 (2017) 1673-1688.
[43] Y. Fan, X. Yin, Q. Xie, Y. Xia, Z. Wang, J. Song, Y. Zhou, X. Jiang, Co-expression of SpSOS1 and SpAHA1 in transgenic Arabidopsis plants improves salinity tolerance, BMC plant biology, 19 (2019) 74.
[44] J.P. An, J.F. Yao, R.R. Xu, C.X. You, X.F. Wang, Y.J. Hao, An apple NAC transcription factor enhances salt stress tolerance by modulating the ethylene response, Physiologia plantarum, 164 (2018) 279-289.
[45] Q.J. Ma, M.H. Sun, H. Kang, J. Lu, C.X. You, Y.J. Hao, A CIPK protein kinase targets sucrose transporter MdSUT2. 2 at Ser254 for phosphorylation to enhance salt tolerance, Plant, cell & environment, 42 (2019) 918-930.
[46] Y. Song, J. Li, Y. Sui, G. Han, Y. Zhang, S. Guo, N. Sui, The sweet sorghum SbWRKY50 is negatively involved in salt response by regulating ion homeostasis,

Plant Molecular Biology, 102 (2020) 603-614.

[47] H. Yan, H. Jia, X. Chen, L. Hao, H. An, X. Guo, The cotton WRKY transcription factor GhWRKY17 functions in drought and salt stress in transgenic Nicotiana benthamiana through ABA signaling and the modulation of reactive oxygen species production, Plant and Cell Physiology, 55 (2014) 2060-2076.

[48] Q.J. Wang, H. Sun, Q.L. Dong, T.Y. Sun, Z.X. Jin, Y.J. Hao, Y.X. Yao, The enhancement of tolerance to salt and cold stresses by modifying the redox state and salicylic acid content via the cytosolic malate dehydrogenase gene in transgenic apple plants, Plant biotechnology journal, 14 (2016) 1986-1997.

[49] D. Wei, W. Zhang, C. Wang, Q. Meng, G. Li, T.H. Chen, X. Yang, Genetic engineering of the biosynthesis of glycinebetaine leads to alleviate salt-induced potassium efflux and enhances salt tolerance in tomato plants, Plant Science, 257 (2017) 74-83.

[50] X.P. Shi, J.J. Ren, Q. Yu, S.M. Zhou, Q.P. Ren, L.J. Kong, X.L. Wang, Overexpression of SDH confers tolerance to salt and osmotic stress, but decreases ABA sensitivity in Arabidopsis, Plant Biology, 20 (2018) 327-337.

[51] J. Zhang, Q. Guo, Y. Feng, F. Li, J. Gong, Z. Fan, W. Wang, Manipulation of monoubiquitin improves salt tolerance in transgenic tobacco, Plant Biology, 14 (2012) 315-324.

[52] Q.Y. Zhang, L.Y. Wang, F.Y. Kong, Y.S. Deng, B. Li, Q.W. Meng, Constitutive accumulation of zeaxanthin in tomato alleviates salt stress- induced photoinhibition and photooxidation, Physiologia Plantarum, 146 (2012) 363-373.

[53] C. Lu, M.-X. Chen, R. Liu, L. Zhang, X. Hou, S. Liu, X. Ding, Y. Jiang, J. Xu, X. Zhao, Abscisic acid regulates auxin distribution to mediate maize lateral root development under salt stress, Frontiers in plant science, 10 (2019) 716.

[54] E. Gnansounou, A. Dauriat, C.E. Wyman, Refining sweet sorghum to ethanol and sugar: economic trade-offs in the context of North China, Bioresource Technology, 96 (2005) 985-1002.

[55] Z. Yang, J.-L. Li, L.-N. Liu, Q. Xie, N. Sui, Photosynthetic Regulation Under Salt Stress and Salt-Tolerance Mechanism of Sweet Sorghum, Frontiers in Plant

Science, 10 (2020) 1722.

[56] F. Sunseri, D. Palazzo, N. Montemurro, F. Montemurro, Salinity tolerance in sweet sorghum (Sorghum bicolor L. Moench): Field performance under salt stress, Ital J Agron, 2 (1998) 111-116.

[57] I. Vasilakoglou, K. Dhima, N. Karagiannidis, T. Gatsis, Sweet sorghum productivity for biofuels under increased soil salinity and reduced irrigation, Field Crops Research, 120 (2011) 38-46.

[58] Z. Yang, Y. Wang, X. Wei, X. Zhao, B. Wang, N. Sui, Transcription profiles of genes related to hormonal regulations under salt stress in sweet sorghum, Plant Molecular Biology Reporter, 35 (2017) 586-599.

[59] N. Sui, Z. Yang, M. Liu, B. Wang, Identification and transcriptomic profiling of genes involved in increasing sugar content during salt stress in sweet sorghum leaves, BMC Genomics, 16 (2015) 534.

[60] Z. Yang, H. Zheng, X. Wei, J. Song, B. Wang, N. Sui, Transcriptome analysis of sweet Sorghum inbred lines differing in salt tolerance provides novel insights into salt exclusion by roots, Plant and Soil, 430 (2018) 423-439.

[61] D. Kim, B. Langmead, S.L. Salzberg, HISAT: a fast spliced aligner with low memory requirements, Nature Methods, 12 (2015) 357.

[62] J. Meng, Z. Lu, H. Liu, L. Zhang, S. Zhang, Y. Chen, M.K. Rao, Y. Huang, A protocol for RNA methylation differential analysis with MeRIP-Seq data and exomePeak R/Bioconductor package, Methods, 69 (2014) 274-281.

[63] G. Yu, L.-G. Wang, Q.-Y. He, ChIPseeker: an R/Bioconductor package for ChIP peak annotation, comparison and visualization, Bioinformatics, 31 (2015) 2382-2383.

[64] M. Pertea, G.M. Pertea, C.M. Antonescu, T.-C. Chang, J.T. Mendell, S.L. Salzberg, StringTie enables improved reconstruction of a transcriptome from RNA-seq reads, Nature biotechnology, 33 (2015) 290.

[65] M.D. Robinson, D.J. McCarthy, G.K. Smyth, edgeR: a Bioconductor package for differential expression analysis of digital gene expression data, Bioinformatics, 26 (2010) 139-140.

[66] N. Sui, S. Tian, W. Wang, M. Wang, H. Fan, Overexpression of

glycerol-3-phosphate acyltransferase from Suaeda salsa improves salt tolerance in Arabidopsis, Frontiers in plant science, 8 (2017) 1337.

[67] B. Zhao, T.T. Wu, S.S. Ma, D.J. Jiang, X.M. Bie, N. Sui, X.S. Zhang, F. Wang, TaD27- B gene controls the tiller number in hexaploid wheat, Plant biotechnology journal, (2019).

[68] C.N. Giannopolitis, S.K. Ries, Superoxide Dismutases, I. Occurrence in Higher Plants, 59 (1977) 309-314.

[69] A. Conesa, S. Götz, J.M. García-Gómez, J. Terol, M. Talón, M. Robles, Blast2GO: a universal tool for annotation, visualization and analysis in functional genomics research, Bioinformatics, 21 (2005) 3674-3676.

[70] J. Ye, L. Fang, H. Zheng, Y. Zhang, J. Chen, Z. Zhang, J. Wang, S. Li, R. Li, L. Bolund, J. Wang, WEGO: a web tool for plotting GO annotations, Nucleic Acids Research, 34 (2006) W293-W297.

[71] R.L. Tatusov, M.Y. Galperin, D.A. Natale, E.V. Koonin, The COG database: a tool for genome-scale analysis of protein functions and evolution, Nucleic Acids Research, 28 (2000) 33-36.

[72] M. Kanehisa, S. Goto, S. Kawashima, Y. Okuno, M. Hattori, The KEGG resource for deciphering the genome, Nucleic Acids Research, 32 (2004) D277-D280.

[73] S. Geula, S. Moshitch-Moshkovitz, D. Dominissini, A.A. Mansour, N. Kol, M. Salmon-Divon, V. Hershkovitz, E. Peer, N. Mor, Y.S. Manor, M.S. Ben-Haim, E. Eyal, S. Yunger, Y. Pinto, D.A. Jaitin, S. Viukov, Y. Rais, V. Krupalnik, E. Chomsky, M. Zerbib, I. Maza, Y. Rechavi, R. Massarwa, S. Hanna, I. Amit, E.Y. Levanon, N. Amariglio, N. Stern-Ginossar, N. Novershtern, G. Rechavi, J.H. Hanna, m^6A mRNA methylation facilitates resolution of naïve pluripotency toward differentiation, Science, 347 (2015) 1002-1006.

[74] C. Bazakos, M.E. Manioudaki, I. Therios, D. Voyiatzis, D. Kafetzopoulos, T. Awada, P. Kalaitzis, Comparative transcriptome analysis of two olive cultivars in response to NaCl-stress, PLOS ONE, 7 (2012) e42931.

[75] X. Du, G. Wang, J. Ji, L. Shi, C. Guan, C. Jin, Comparative transcriptome analysis of transcription factors in different maize varieties under salt stress

conditions, Plant Growth Regulation, 81 (2017) 183-195.

[76] M. Quint, L.S. Barkawi, K.-T. Fan, J.D. Cohen, W.M. Gray, Arabidopsis IAR4 Modulates Auxin Response by Regulating Auxin Homeostasis, Plant Physiology, 150 (2009) 748-758.

[77] Y. Fu, Y. Yang, S. Chen, N. Ning, H. Hu, Arabidopsis IAR4 Modulates Primary Root Growth Under Salt Stress Through ROS-Mediated Modulation of Auxin Distribution, Front Plant Sci, 10 (2019) 522.

[78] C.-Z. Chen, X.-F. Lv, J.-Y. Li, H.-Y. Yi, J.-M. Gong, Arabidopsis NRT1. 5 is another essential component in the regulation of nitrate reallocation and stress tolerance, Plant Physiology, 159 (2012) 1582-1590.

[79] H. Li, M. Yu, X.-Q. Du, Z.-F. Wang, W.-H. Wu, F.J. Quintero, X.-H. Jin, H.-D. Li, Y. Wang, NRT1. 5/NPF7. 3 functions as a proton-coupled H+/K+ antiporter for K+ loading into the xylem in Arabidopsis, The Plant Cell, 29 (2017) 2016-2026.

[80] J. Luo, Y. Wang, M. Wang, L. Zhang, H. Peng, Y. Zhou, G. Jia, Y. He, Natural variation in RNA m^6A methylation and its relationship with translational status, Plant Physiology, (2020) pp.00987.02019.

[81] Z. Miao, T. Zhang, Y. Qi, J. Song, Z. Han, C. Ma, Evolution of the RNA N^6-methyladenosine methylome mediated by genomic duplication, Plant Physiology, (2020) pp.00323.02019.

[82] R.A. Gaxiola, J. Li, S. Undurraga, L.M. Dang, G.J. Allen, S.L. Alper, G.R. Fink, Drought-and salt-tolerant plants result from overexpression of the AVP1 H+-pump, Proceedings of the National Academy of Sciences, 98 (2001) 11444-11449.

[83] M. Ashraf, Organic substances responsible for salt tolerance inEruca sativa, Biol. Plant., 36 (1994) 255-259.

[84] G. Feng, F.S. Zhang, X.L. Li, C.Y. Tian, C. Tang, Z. Rengel, Improved tolerance of maize plants to salt stress by arbuscular mycorrhiza is related to higher accumulation of soluble sugars in roots, Mycorrhiza, 12 (2002) 185-190.

[85] R.J. Ries, S. Zaccara, P. Klein, A. Olarerin-George, S. Namkoong, B.F. Pickering, D.P. Patil, H. Kwak, J.H. Lee, S.R. Jaffrey, m^6A enhances the phase separation potential of mRNA, Nature, (2019).

[86] S.H. Ok, H.J. Jeong, J.M. Bae, J.-S. Shin, S. Luan, K.-N. Kim, Novel CIPK1-associated proteins in *Arabidopsis* contain an evolutionarily conserved C-terminal region that mediates nuclear localization, Plant Physiology, 139 (2005) 138.

[87] K.-N. Kim, Y.H. Cheong, R. Gupta, S. Luan, Interaction specificity of *Arabidopsis* calcineurin B-Like calcium sensors and their target kinases, Plant Physiology, 124 (2000) 1844.

[88] Ü. Kolukisaoglu, S. Weinl, D. Blazevic, O. Batistic, J. Kudla, Calcium sensors and their interacting protein kinases: genomics of the *Arabidopsis* and rice CBL-CIPK signaling networks, Plant Physiology, 134 (2004) 43.

[89] J. Li, H. Yang, W.A. Peer, G. Richter, J. Blakeslee, A. Bandyopadhyay, B. Titapiwantakun, S. Undurraga, M. Khodakovskaya, E.L. Richards, Arabidopsis H+-PPase AVP1 regulates auxin-mediated organ development, Science, 310 (2005) 121-125.

[90] E.K. Brauer, N. Ahsan, R. Dale, N. Kato, A.E. Coluccio, M.A. Piñeros, L.V. Kochian, J.J. Thelen, S.C. Popescu, The Raf-like kinase ILK1 and the high affinity K+ transporter HAK5 are required for innate immunity and abiotic stress response, Plant physiology, 171 (2016) 1470-1484.

[91] F. Roudier, A.G. Fernandez, M. Fujita, R. Himmelspach, G.H.H. Borner, G. Schindelman, S. Song, T.I. Baskin, P. Dupree, G.O. Wasteneys, P.N. Benfey, COBRA, an Arabidopsis Extracellular Glycosyl-Phosphatidyl Inositol-Anchored Protein, Specifically Controls Highly Anisotropic Expansion through Its Involvement in Cellulose Microfibril Orientation, The Plant Cell, 17 (2005) 1749-1763.

Figure legends

Fig. 1. Overview of m^{6}A modification in sweet sorghum. (a) Schematic diagram of m^{6}A-seq and RNA-seq. The salt-tolerant genotype M-81E and the salt-sensitive genotype Roma were treated with 150 mmol NaCl for 0 h and 24 h, respectively, and roots were collected for m^{6}A-seq and RNA-seq. NGS, next-generation sequencing. (b) The number of m^{6}A peaks detected in M_CK and R_CK. (c) Significant (p value<1e-5; chi-square test) overlap of m^{6}A peaks between M_CK and R_CK. (d) The gene ontology (GO) analysis for the common m^{6}A peaks between M_CK and R_CK.

Fig. 2. Characteristics and extent of the m^{6}A modification in sweet sorghum roots. (a) Sequence logo representing the most common consensus motif (RRm^{6}ACH) in the m^{6}A peaks in sweet sorghum. (b) Percentage of total m^{6}A peaks located throughout regions of mRNA transcripts within M_CK and R_CK. Each transcript is divided into three parts: 5' UTRs, CDs, and 3' UTRs. (c) Percentage of M_CK and R_CK the first 1000 m^{6}A peaks at different positions in the transcript. (d) The ratio of mRNA expression levels (FPKM) in two samples containing region-specific m^{6}A peaks. The gene expression levels (FPKM) in different biological replicates are averaged, and then log10 (FPKM+1) is calculated to avoid calculating log10 (0). Genes are divided into three categories (5' UTRs, CDs, and 3' UTRs) according to the peak positions.

Fig. 3. Analysis of m^{6}A peaks in M-81E under salt stress. (a) Overlap of m^{6}A peaks between M_CK and M_S, p value<1e-5. (b) The number of significant m^{6}A peaks and DEGs between M_S and M_CK. p-value of the peak<1e-5, log2 (fold change of the peak) ≥1 or log2 (fold change of the peak) ≤-1. DEGs fold changes≧2, p-value ≤ 0.05. (c) Overlap of significant m^{6}A peak and DEGs between M_CK and M_S. There are overlapping genes between m^{6}A up and m^{6}A down, it is because of different genomic regions within the same gene show both m^{6}A down and m^{6}A up. (d) The KEGG enrichment scatters plot display significantly different m^{6}A peaks or DEGs

assigned to different KEGG pathways. (e) The GO analysis for the specific m^{6}A peaks between M_S and M_CK. The heat map displays significantly different m^{6}A peaks assigned to different GO terms. The GO terms shown are significantly enriched, and we have displayed more GO terms related to the biological process in limited pictures. Red indicates that more genes are enriched in these GO terms.

Fig. 4. Analysis of m^{6}A peaks in Roma under salt stress. (a) Overlap of m^{6}A peaks between R_CK and R_S, p value<1e-5. (b) The number of significant m^{6}A peaks and DEGs between R_S and R_CK. p-value of the peak<1e-5, log2 (fold change of the peak) ≥1 or log2 (fold change of the peak) ≤-1. DEGs fold changes≧2, p-value ≤ 0.05. (c) Overlap of significant m^{6}A peak and DEGs between R_S and R_CK. There are overlapping genes between m^{6}A up and m^{6}A down, it is because of different genomic regions within the same gene show both m^{6}A down and m^{6}A up. (d) The GO analysis for the specific m^{6}A peaks between R_S and R_CK. The heat map displays Significantly different m^{6}A peaks assigned to different GO terms. The GO terms shown are significantly enriched. Red indicates that more genes are enriched in these GO terms.

Fig. 5. The effect of m^{6}A modification on mRNA abundance (a) Representative Integrative Genomics Viewer (IGV) plot showing dynamic m^{6}A peaks in Roma under salt stress. The different colors showed the accumulation of m^{6}A-IP peaks from two accessions. Blue represents m^{6}A-input peaks and pink represents m^{6}A-IP peaks. (b) Percent of transcripts remaining 24 hr post-treatment with transcription inhibitors in R_CK and R_S.

Fig. 6. Analysis of the difference m^{6}A peaks between M-81E and Roma. (a) The number of significant m^{6}A peaks and DEGs between M_CK and R_CK. p-value of the peak<1e-5, log2 (fold change of the peak) ≥1 or log2 (fold change of the peak) ≤-1. DEGs fold changes≧2, p-value ≤ 0.05. (b) Overlap of significant m^{6}A peak and DEGs between M_CK and R_CK. There are overlapping genes between m^{6}A up

and m^{6}A down, it is because of different genomic regions within the same gene show both m^{6}A down and m^{6}A up. (c) The KEGG enrichment scatters plot display significantly different m^{6}A peaks or DEGs assigned to different KEGG pathways. (d) The GO analysis for the specific m^{6}A peaks between M_CK and R_CK. The heat map displays Significantly different m^{6}A peaks assigned to different GO terms. The GO terms shown are significantly enriched, and we have displayed more GO terms related to the biological process in limited pictures. Red indicates that more genes are enriched in these GO terms.

Supporting information

Fig. S1 Reads density plots of M-81E and Roma in IP and input under normal and salt treatment conditions. m^{6}A peaks were mapped back to the corresponding gene and assigned as originated from 5'UTR, CDS, and 3'UTR.

Fig. S2 The KEGG enrichment scatter plot display of significantly different m^{6}A peaks or DEGs assigned to different KEGG pathways. p-value of the peak<1e-5, log2 (fold change of the peak) ≥1 or log2 (fold change of the peak) ≤-1. DEGs fold changes≧2, p-value ≤ 0.05.

Fig. S3 Relative expression levels of writers and erasers genes in the roots of sweet sorghum. The level of gene expression in R_CK as a control.

Fig. S4 Scatter plot of differentially expressed genes in different comparison groups.

Table S1 Primers List. This table contains a list of all primers used for quantitative real-time PCR analysis.

Table S2 The sequenced and mapped reads in the m^{6}A-seq, mRNA-seq, and input RNA-seq samples.

Table S3 M_CK, R_CK, M_S, and R_S m^{6}A peaks. This table contains the locations of high-confidence m^{6}A peaks that overlapped in both replicates of m^{6}A-seq for M_CK, R_CK, M_S, and R_S. And the GO analyses of the m^{6}A-containing of M_CK, R_CK, M_S, and R_S.

Table S4 The differentially expressed genes and the variations in m^6A modifications between M_CK and R_CK.

Table S5 Gene ID, name codes, and amino acid sequences of m^6A writers and erasers from Sorghum bicolor.

Table1. Transcripts with significantly increased m^6A peaks and mRNA abundance.

Gene ID	Orthologues in *A. thaliana*	m^6A fold_enrchment	m^6A regulation	Gene fold change	Gene regulation	Function annotation	Reference
SORBI_3010G101300	*IAR4*	12.60	up	8.24	up	IAR4 regulates root development through the auxin pathway. Under salt stress, IAR4 regulates the primary growth of roots by integrating the ROS pathway and the auxin pathway;	[76, 77]
SORBI_3004G276200	*NRT1.5*	13.90	up	2.81	up	NRT1.5 plays a crucial role in K^+ translocation from root to shoot, and is also involved in the coordination of K^+/NO^{3-} distribution in plants, and participates in the regulation of plant stress tolerance.	[78, 79]
SORBI_3004G068300	*AVP1*	2.20	up	2.03	up	AVP1 increasing the vacuolar proton gradient results in increased solute accumulation and water retention under salt stress.	[82, 89]
SORBI_3003G385000	*ILK1*	1.96	up	3.32	up	ILK1 was a putative H^+/K^+ symporter that mediates a high-affinity uptake during K^+ deficiency.	[90]
SORBI_3002G368100	*Cob*	76.10	up	3.00	up	COB is primarily implicated in microfibril deposition during rapid elongation, and it is an essential factor in highly anisotropic expansion during plant morphogenesis.	[91]

Figure 1

Click here to access/download;Figure;Figure 1.tif

Fig. 1

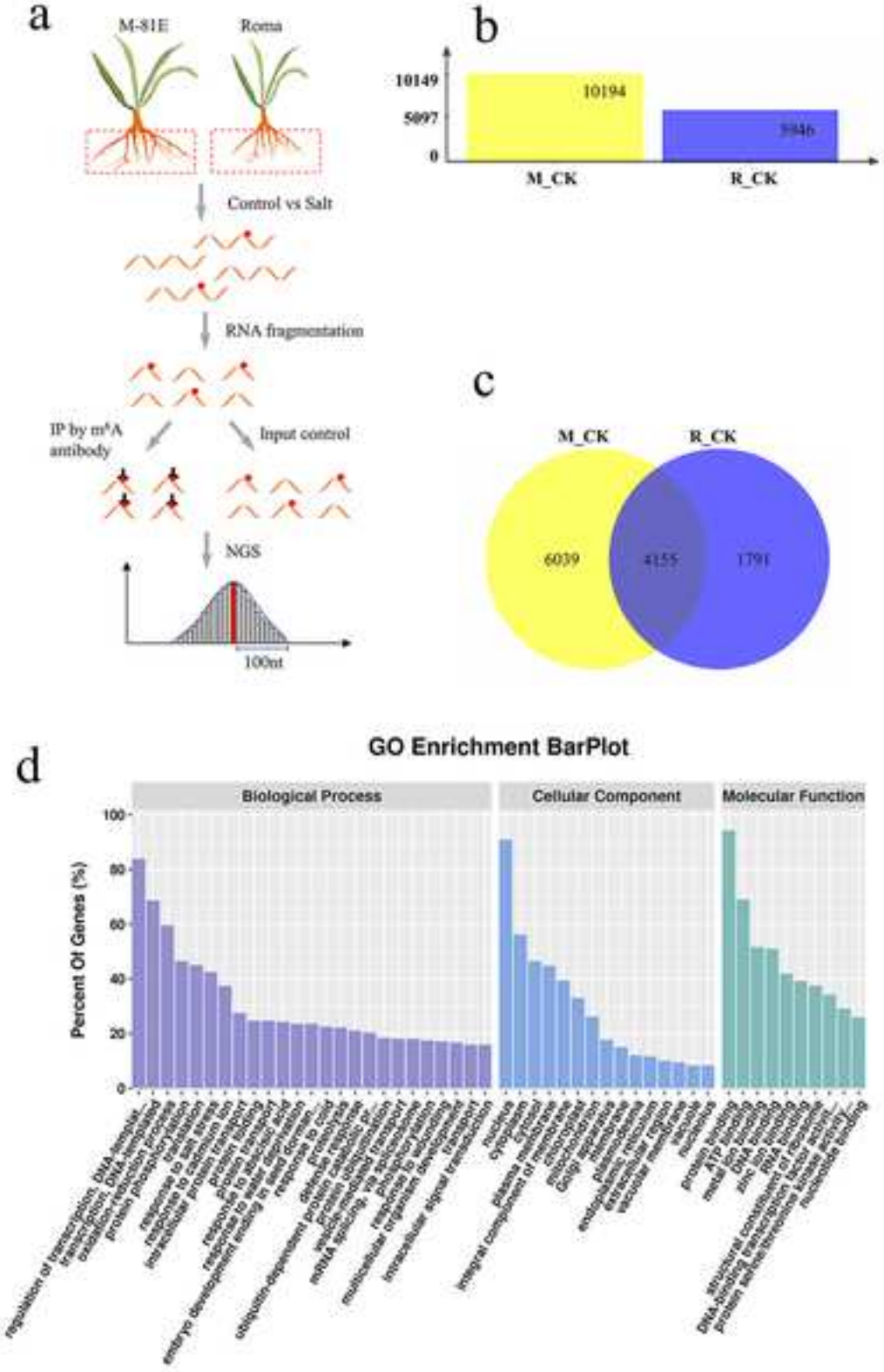

Fig. 2

a

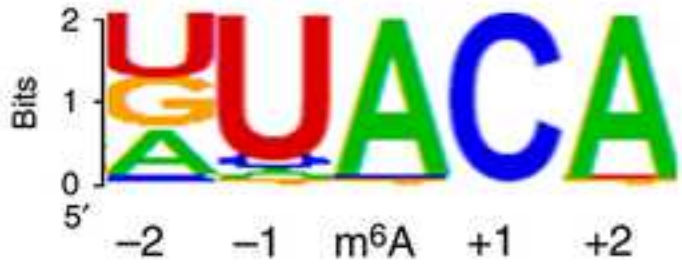

b

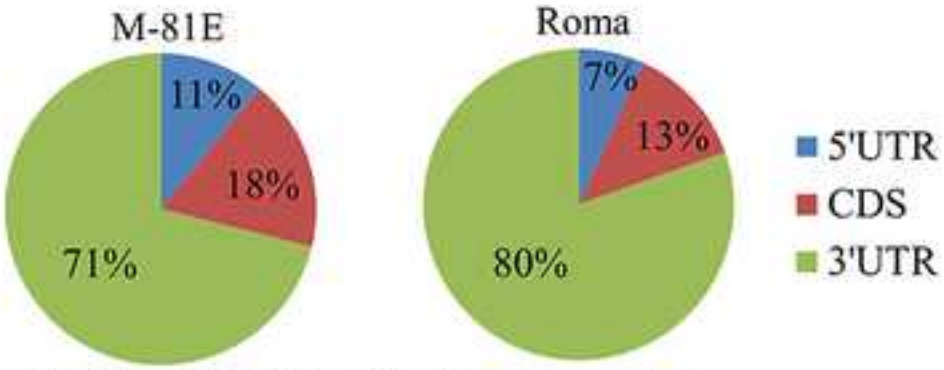

All m⁶A peak distribution within different gene contexts

c

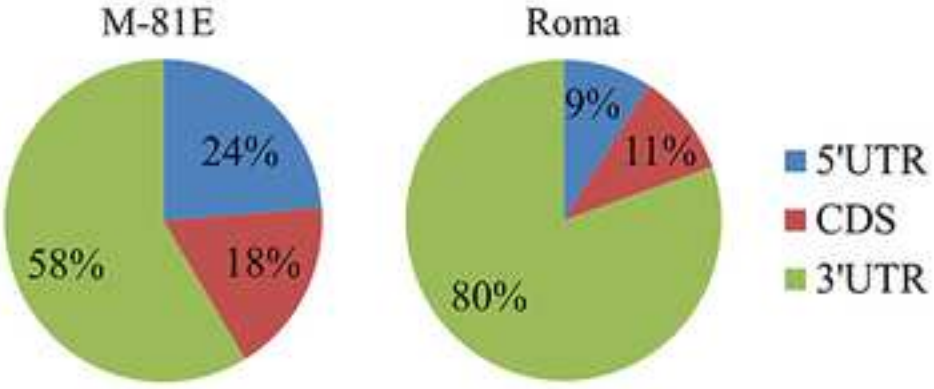

Top 1000 m⁶A peak distribution within different gene contexts

d

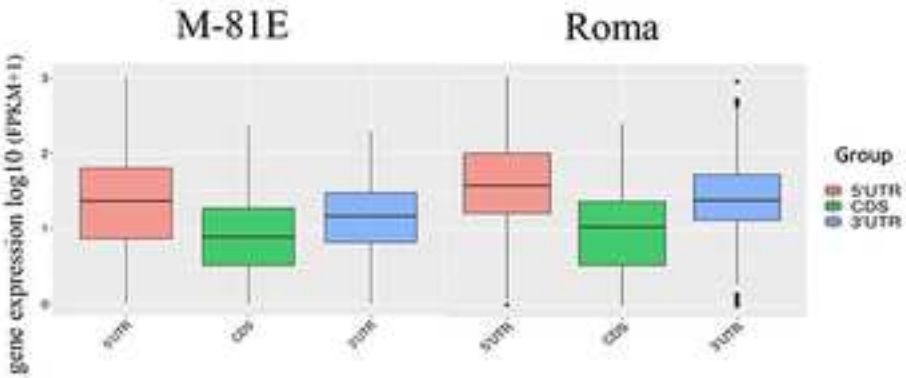

Figure 3

Click here to access/download;Figure;Figure 3.tif

Fig. 3

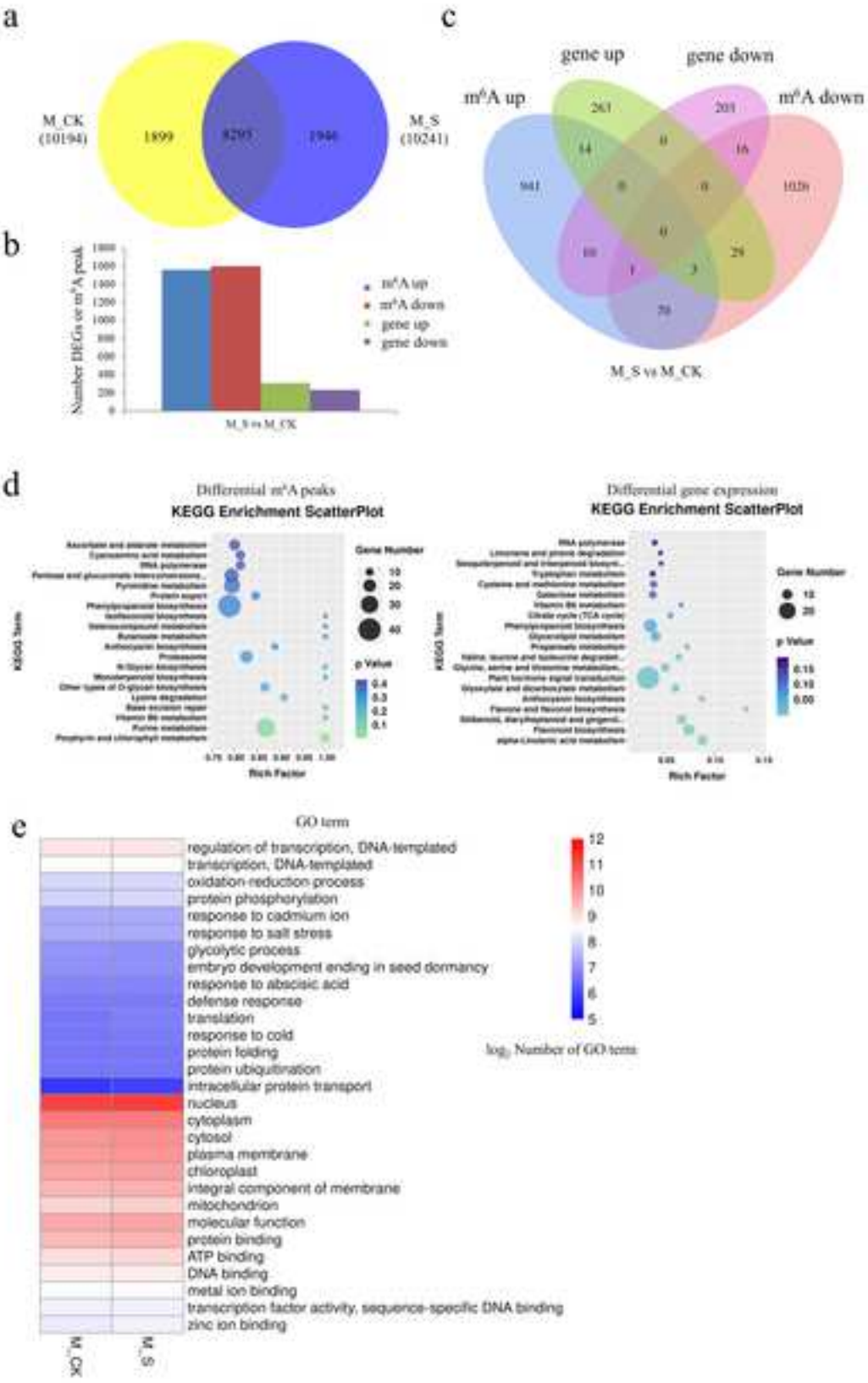

Fig. 4

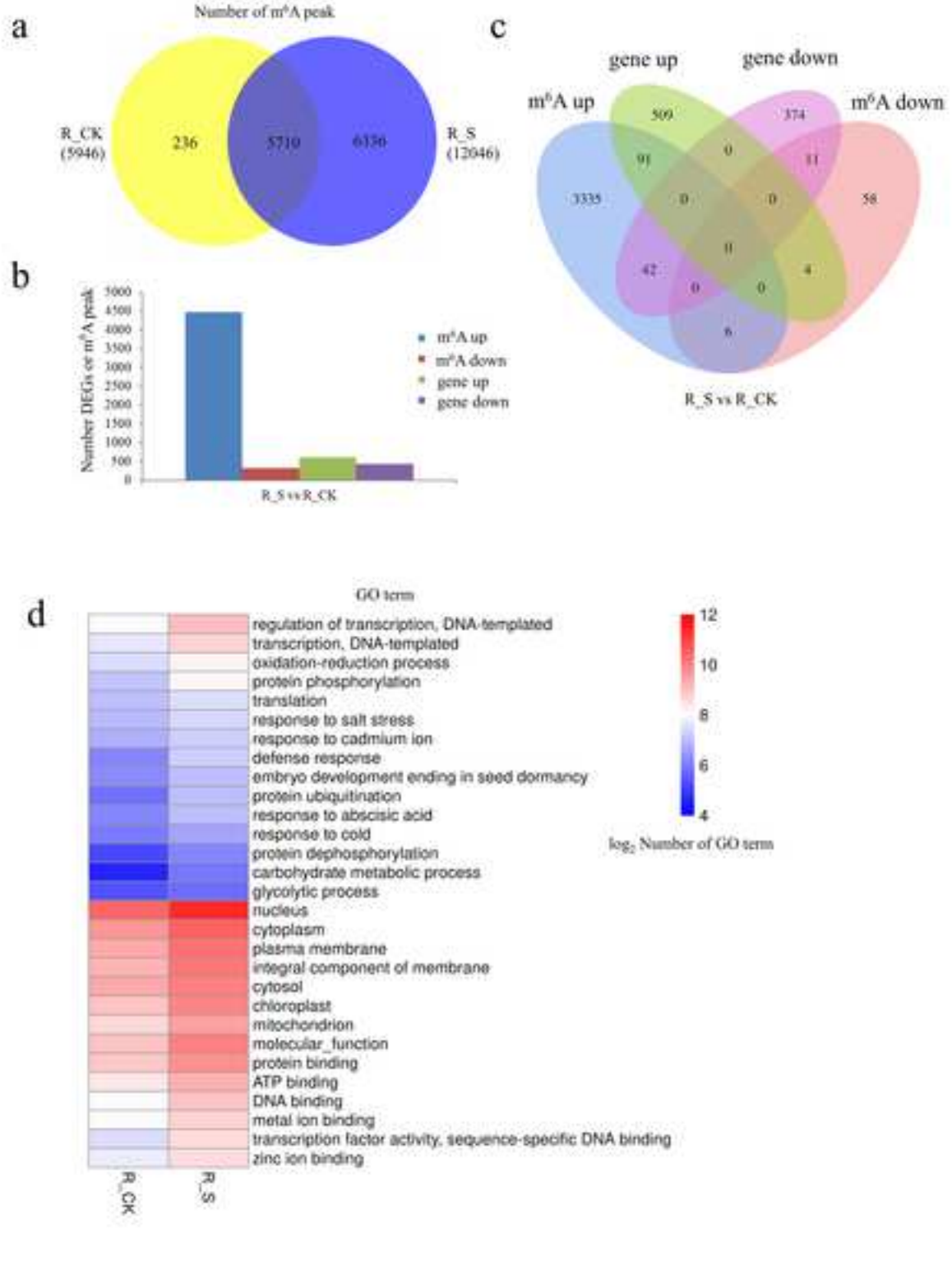

Fig. 5

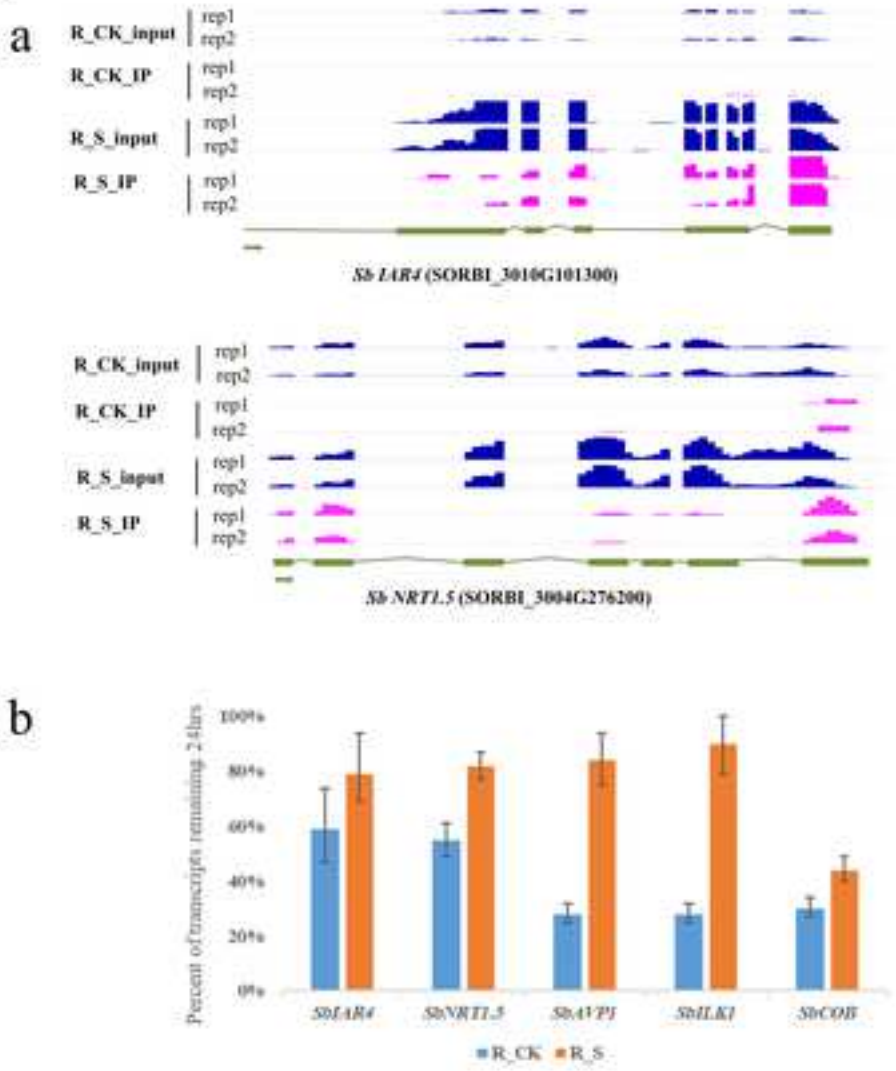

Figure 6

Click here to access/download;Figure;Figure 6.tif

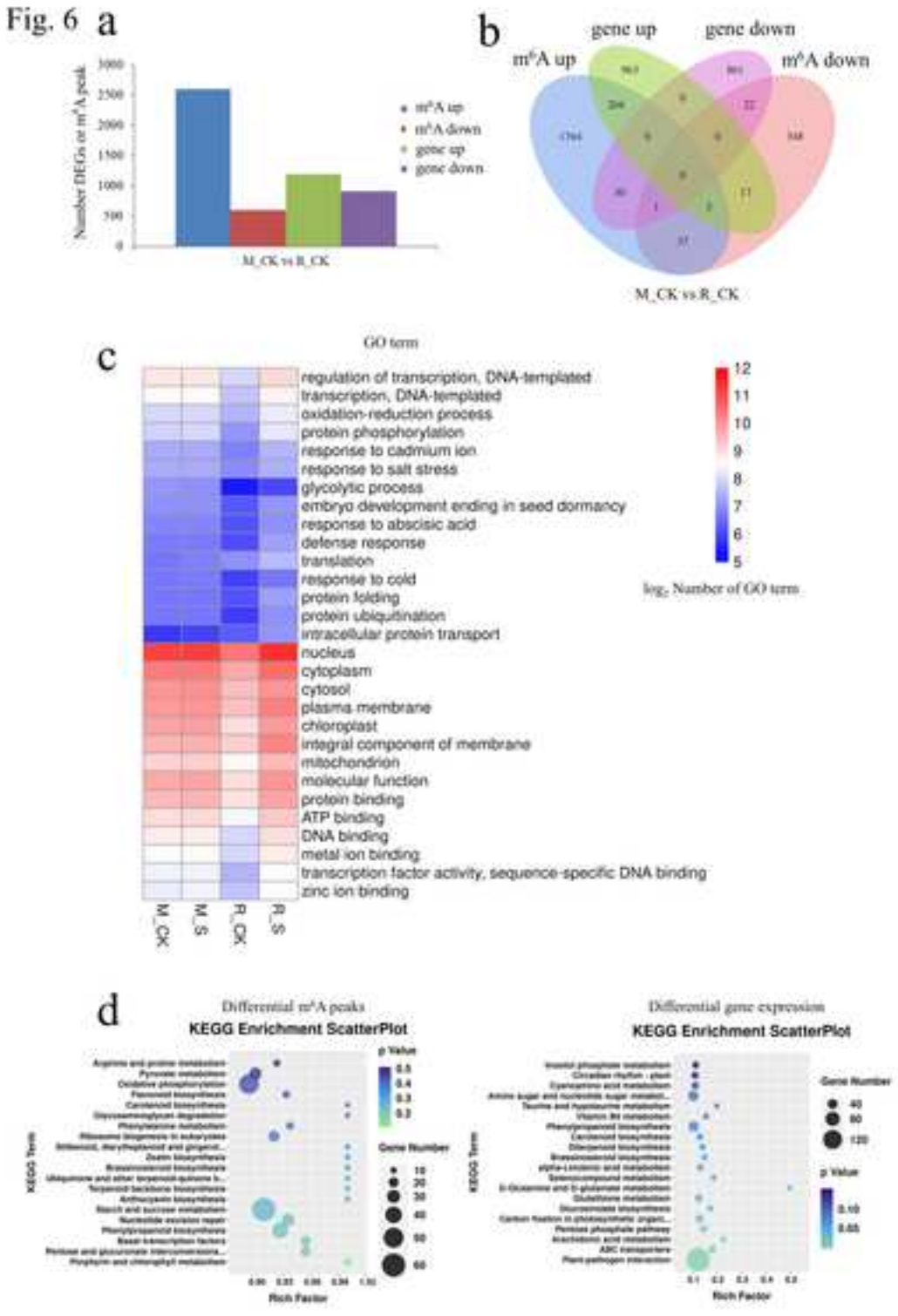

Fig. S1

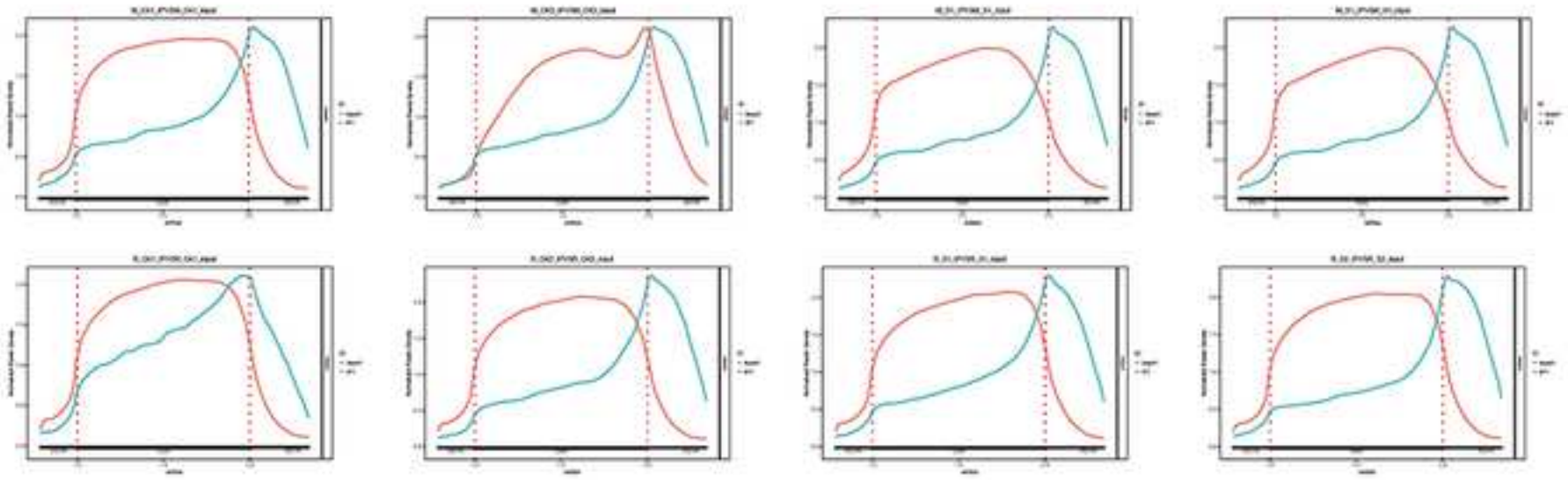

Fig. S2

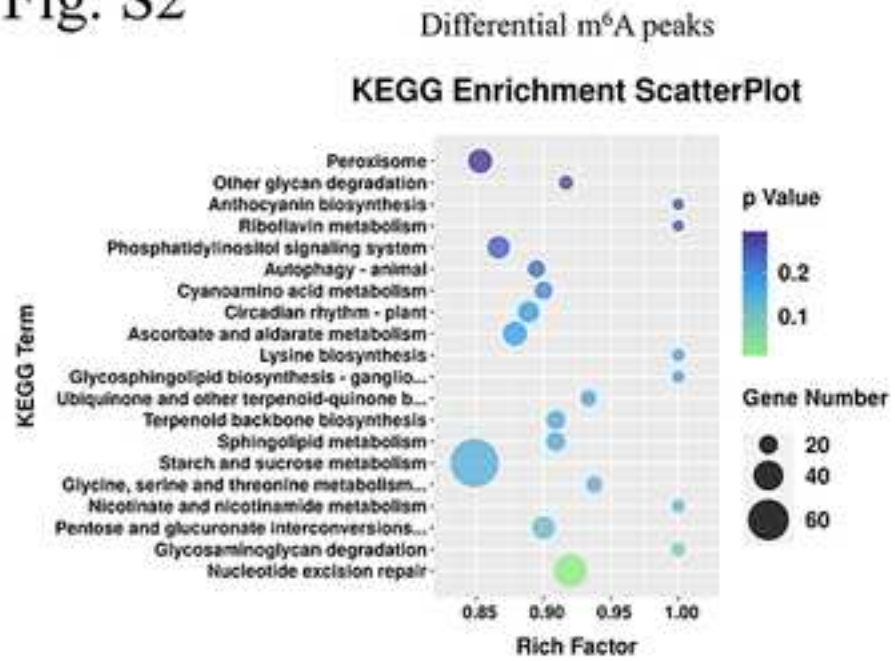

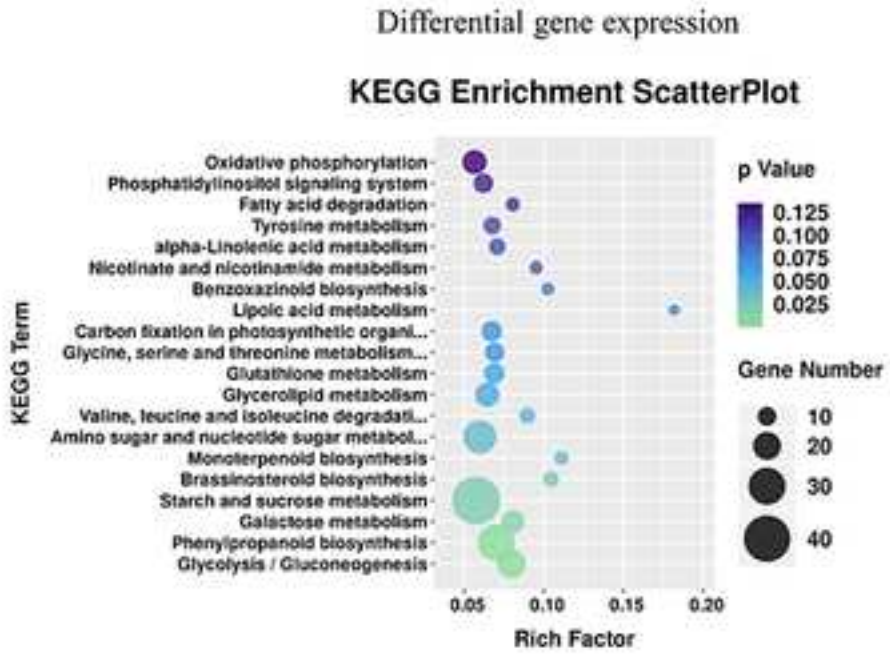

Fig. S3

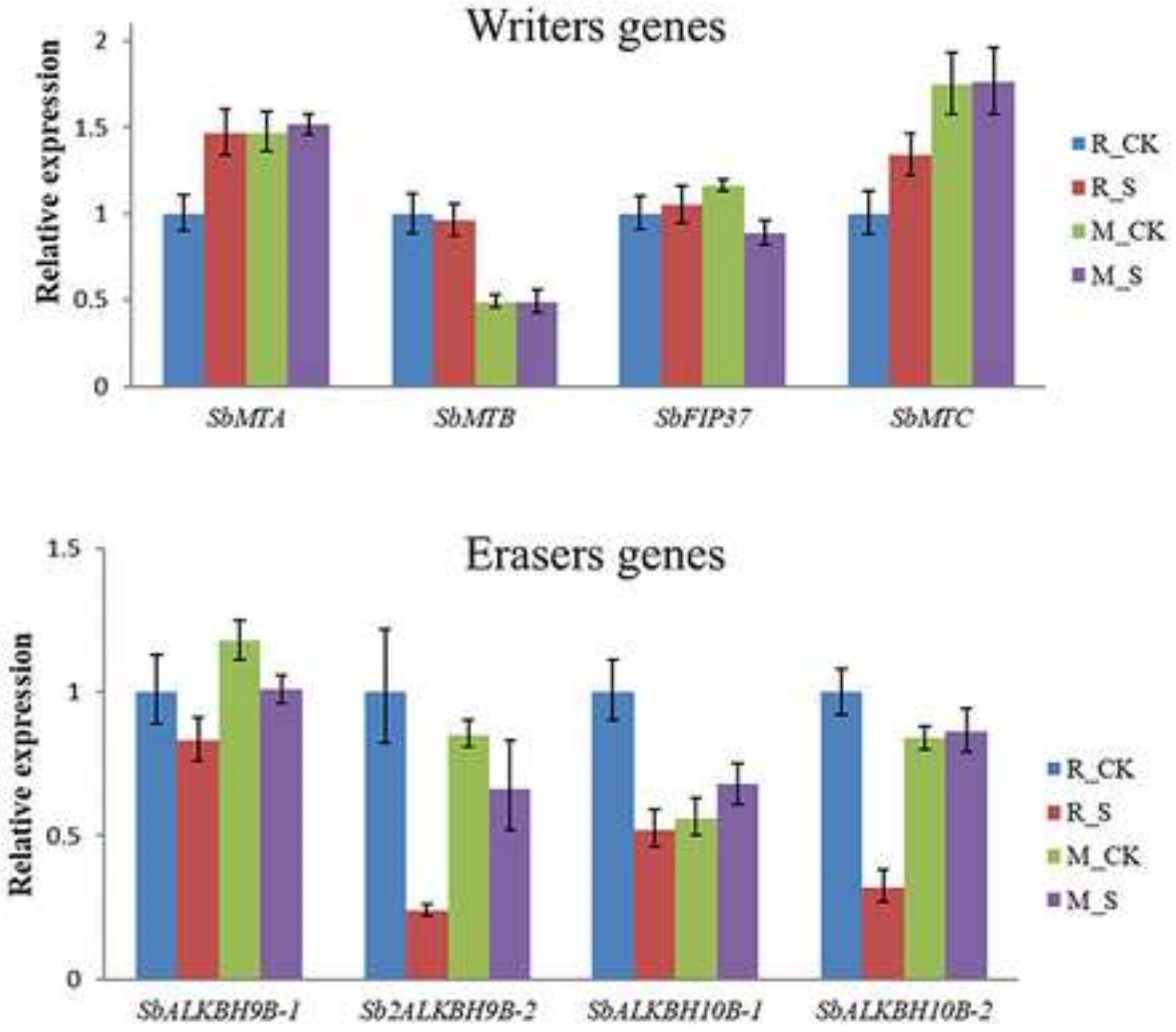

Fig. S4

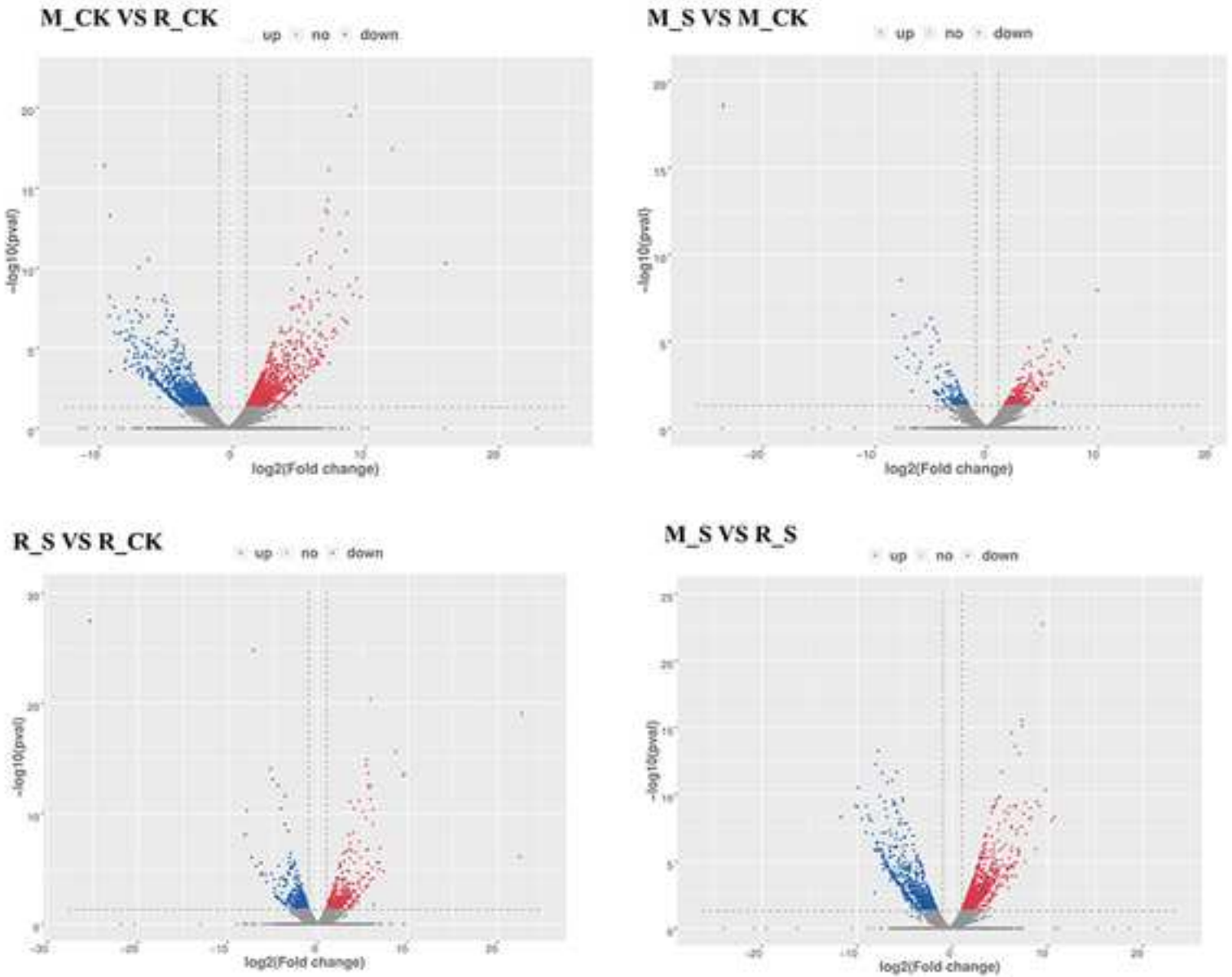

Supplementary Table S1: List primers used in this study

Gene ID	Name codes	Forward primer
SORBI_3001G11260	Sbactin-1	ACGGCCTGGATGGCGACGTACAT
SORBI_3004G28500	SbMTA	GCTCGAACTCATCGGCTCTC
SORBI_3001G50390	SbMTB	TCAGACAGAGGGAGGGACAG
SORBI_3004G01830	SbMTC	GGCTCCTTAGCATCTCGCAA
SORBI_3004G03310	SbFIP37	AGTCCGTGGAGCCCTATGAG
SORBI_3010G02880	SbALKBH9B-1	GTGTTCCAGCAGTCCCTACC
SORBI_3006G27860	SbALKBH9B-2	TACAAGAGCACAAGCAGGGC
SORBI_3009G13090	SbALKBH10B-	GACCACCTTGTTCTTTGGCG
SORBI_3001G44180	SbALKBH10B-	TCTCGCAACTGGGTCACTT
SORBI_3010G10130	SbIAR4	AACGGCCCAAGAGCTAAAGG
SORBI_3004G27620	SbNRT1.5	CAGGACAAGTGCTGCGAGTA
SORBI_3004G06830	SbAVP1	GAAGACAGTGCAAAGCTGGC
SORBI_3003G38500	SbILK1	TTCAGCTACCACACTGCACC
SORBI_3002G36810	SbCob	AACCAACATCCCCCATTGCT

Reverse primer
GCAGAAGGACGCCTACGTTGGTGAC
GTACAGCGTAGGGACGAAGG
GGCTCCTTAGCATCTCGCAA
CCTGTTCCAATGTCAAAGCCC
GCTGATCTTGCGCGTTTCTT
GAGGGGCAAGGTTAAGCAGT
CCGAGAGCCGGAAAGTCATC
TGTAGTTGCCGTTGCTGTCA
GGGATGGCGGGAGATGTTAG

TCAGATGGGTCAGGCATTGG
CCACTTGCTGACGTTGTTGG
TGTAACCCAAAGCAAGCCCA
GGCGTCCTCACTGATCCTTC
GTAGTCCCAGCCTGTCCAAC

Table S2 The sequenced and mapped reads in the m^{6}A-seq, mRNA-sec

Sample_ID	Category	Raw_Reads	Valid_Reads	Valid%	Mapped reads
M_CK1_IP	m6A-seq	43493838	43493340	100.00	33570868(77.19%)
M_CK2_IP	m6A-seq	31586878	31582254	99.98	24013493(76.03%)
M_S1_IP	m6A-seq	54641008	54640460	100	39492108(72.28%)
M_S2_IP	m6A-seq	64717676	64712996	99.99	51934605(80.25%)
R_CK1_IP	m6A-seq	28116740	25430902	88.18	17875486(70.29%)
R_CK2_IP	m6A-seq	32414224	32413596	100.00	24395456(75.26%)
R_S1_IP	m6A-seq	30201268	30197202	99.98	25526768(84.53%)
R_S2_IP	m6A-seq	37025598	37022026	99.99	30132289(81.39%)
M_CK1	RNA-seq	48011720	47263314	97.79	41606629(88.03%)
M_CK2	RNA-seq	40353032	39552704	97.47	34051026(86.09%)
M_S1	RNA-seq	63221264	61574956	97.15	55199140(89.65%)
M_S2	RNA-seq	42533870	42149026	98.92	38322013(90.92%)
R_CK1	RNA-seq	45405304	44803730	98.35	41593826(92.84%)
R_CK2	RNA-seq	57588240	56619666	97.94	51959939(91.77%)
R_S1	RNA-seq	47525860	46890350	98.29	44009556(93.86%)
R_S2	RNA-seq	38020512	37551118	98.36	34102031(90.81%)

ɟ samples

Q20%	Q30%	GC%
97.96	94.43	50.54
98.01	94.39	49.30
98.14	94.79	50.03
97.99	94.23	48.70
98.18	94.84	51.26
98.79	96.53	49.16
98.05	94.49	49.17
98.22	94.82	48.68
98.81	96.12	52.32
98.63	95.57	45.89
97.40	93.24	53.64
98.85	96.15	51.93
98.83	96.05	51.25
98.72	95.77	51.38
98.76	95.88	51.68
98.74	95.85	51.07